NASA CR-66834

GAS DENSITY DETECTOR

FOR USE IN SPACE

By D. S. Wollan, W. P. Trower,
K. Ramamurti and W. K. Meshejian

Physics Department
Virginia Polytechnic Institute
Blacksburg, Virginia 24061

Prepared under Contract No. NAS1-8145 by
Virginia Polytechnic Institute
Blacksburg, Virginia 24061

for

NATIONAL AERONAUTICS AND SPACE ADMINISTRATION

October 1969

TABLE OF CONTENTS

SUMMARY 1

I. INTRODUCTION 2

II. THEORY 8

A. The Ionization of Gases by Radioactive Sources 8

B. Ionization Chambers 17

C. Proportional Counters 24

D. Glow Tubes 28

III. EXPERIMENTAL PROCEDURE 33

IV. EXPERIMENTAL RESULTS 36

A. Ionization Chambers 36

B. Proportional Counters 42

C. Glow Tubes 46

V. CONCLUSIONS AND RECOMMENDATIONS 57

REFERENCES 59

GAS DENSITY DETECTOR FOR USE IN SPACE*

By D. S. Wollan, W. P. Trower,
K. Ramamurti and W. K. Meshejian

Physics Department
Virginia Polytechnic Institute
Blacksburg, Virginia 24061

SUMMARY

We have investigated theoretically and experimentally the suitability of radioactively-induced currents in ionization chambers and proportional counters and of breakdown currents in glow tubes as a monitor of gas density for meteoroid detection in space. Ionization chambers using moderate ($\lesssim$ 1 mCi) alpha sources have maximum currents $\lesssim 10^{-6}$ A at several hundred volts. The current has an approximate linear dependence on gas density at intermediate densities (~ 1 to 760 Torr at 25° C), which might make it useful as a hole size detector. Proportional counters utilizing similar sources provide currents up to 10^{-4} A at ~ 1000 V, but the dependence of current on gas density is non-monotonic, which would make analysis of their readings difficult. The most promising gas detectors are glow tubes, which have currents ~ 1 mA at moderate voltages (~ 200 V). Optimum parameters for a coaxial glow tube are given. We use helium gas and a 0.34 μCi cobalt-60 radioactive foil source to aid in firing each tube. Three devices have been constructed and calibrated from -195° to 100° C. Vibration tests are reported. Use of a glow tube for meteoroid hole size detection in space may be difficult.

* Preliminary results were reported in Va. J. Sci. 20 (1969).

I. INTRODUCTION

A knowledge of meteoroid characteristics in space is of intrinsic interest to space scientists and has great practical importance to NASA as a design consideration.[1] Measurement of the properties of meteoroids is not an easy task because they have no characteristic electric or magnetic properties, so that usual electromagnetic detection techniques are not possible. One possible detection device is a gas-filled, thin-walled container which loses its gas when punctured by a meteoroid. Unless the puncture is easily repairable, this is clearly a one-shot device. This detector can operate in one of two modes. In the first it is just an "on-off" gauge, signaling that a puncture has occurred if the gas density falls below some preset threshold. A large number of containers must be flown if the average meteoroid flux is to be measured from the number of containers punctured in a given time period and from the geometry of the devices. A second mode is that of a hole size indicator in which the time rate of change of the gas density in the device is measured. The size of a puncture in the container wall could be determined if the relationship between hole size and gas density changes were known. This would be very useful information, but is harder to do.

The purpose of the development work described here is to construct a small, rugged, lightweight gauge for measuring the gas density in a container by using ionizing particles. We concentrate on an "on-off" type gauge. A schematic diagram is shown in Figure 1. Particles produced by radioactive isotopes (i.e. alpha, beta or gamma radiation) ionize the gas between the two electrodes of the gas detector. An emf. ε establishes an electric current I between the electrodes and in the external circuit. The current I, measured with an ammeter or electrometer, is in general a complicated

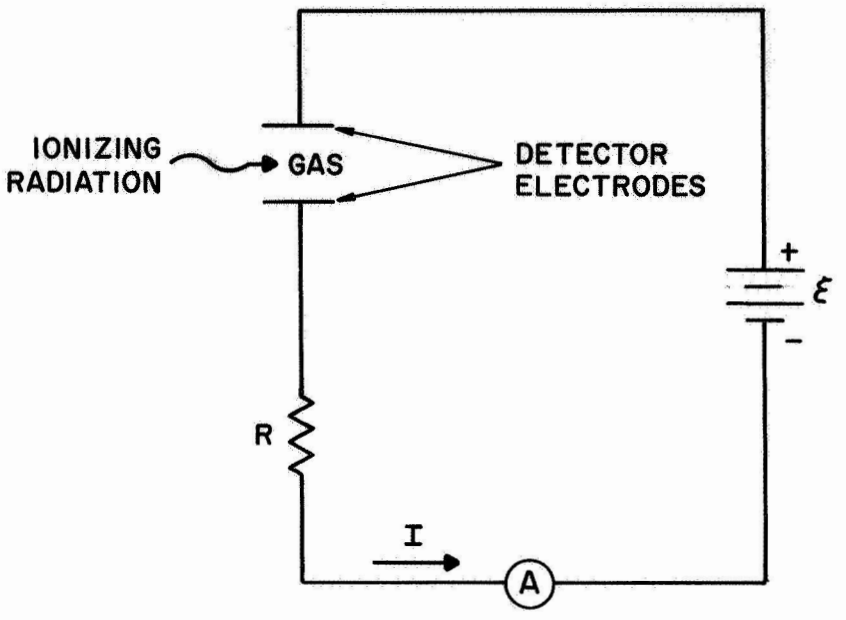

Figure 1. Schematic diagram of a gas detector.

function of the gas density as well as the other parameters, but we note that there is negligible current when the interelectrode volume is highly evacuated, as there are few gas molecules to ionize. A gas density gauge based on this principle can be constructed which has small size and weight, rapid response, and no moving parts. It would give a relatively large current output when gas is present, and a negligible current when there is no gas in the detector.

A typical I-V plot which is characteristic for this device operating on direct current at fixed gas pressure is shown in Figure 2. V is the voltage across the electrodes. The region O to B is known as the "ionization chamber" regime.[2-7] As V is increased from O to A, the current increases because more and more of the ionized gas particles are swept to and collected by the electrodes, and fewer recombine before collection. The constant current from A to B indicates that all the gas ions being produced are collected, as recombination is negligible. In the region B to C the gas ions are accelerated sufficiently by the higher voltages to produce secondary ions in the gas. Hence, there is a "multiplication" effect whereby one ion produced by the incident radiation can itself produce many more ions to be collected by the electrodes. In the lower part of the region B to C, called the "proportional counter" regime,[3-5,7,8] the electric current is not self-maintaining: if the ionizing radiation is removed, the current falls to zero. This is also true for ionization chambers. However, in the upper part of the B to C region, known as the "Geiger-Muller"[9] regime, the current is self-maintaining. Ionizing radiation is needed to begin the electric discharge, but once established, the current will continue in the absence of the radiation. Geiger-Muller counters operate in this regime

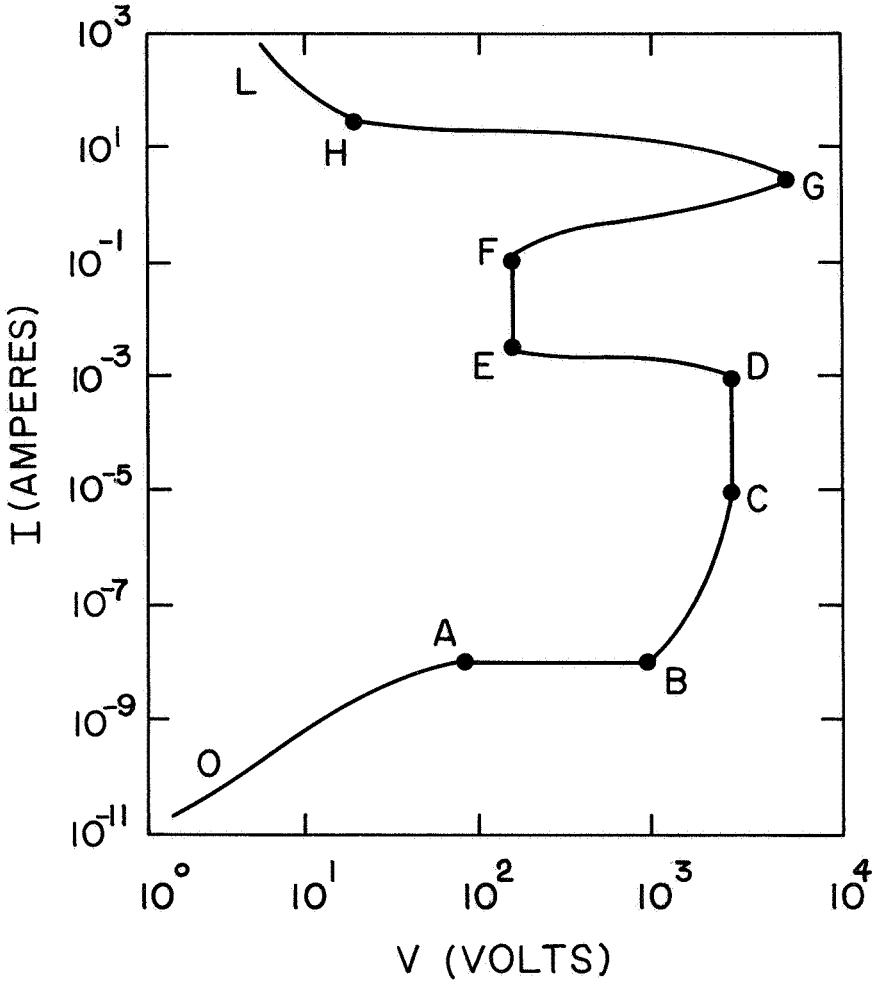

Figure 2. Typical current-voltage characteristics of a gas detector at fixed gas density.

with suitable quenching agents.

The regions from C to L in Figure 2 are all self-maintaining. The "Townsend discharge" region C to D is used for "corona stabilizer" tubes.[10] "Glow discharge"[10-14] occurs in the region D to G. The constant voltage, "normal glow discharge" regime from E to F is the operating region for commercial glow lamps and voltage regulator tubes. From G to L, there is a transition to a high current arc discharge. It is worth mentioning that the current is limited principally by the external resistance (R in Figure 1) in the glow discharge and arc regions.

We have examined the ionization chamber, proportional counter, and glow discharge regimes for their suitability as a gas detector. The first two involve relatively simple construction techniques because gas purity and the cleanliness of the electrode surfaces are not of critical concern. Unfortunately, the ionization chamber gives low currents (~ 10^{-7} A) when moderate source activities are used. The proportional counter on the other hand requires high voltages (> 1000 V). The glow tube operating in the normal glow discharge region, gives acceptable currents (~ 1 mA) at moderately low voltages (~ 200 V), but the gas purity and surface cleanliness requirements are extremely stringent for consistent optimum results.

In what follows we give a summary of the key theoretical ideas needed to understand gas detectors. The interested reader should consult the references for detailed derivations and a more complete discussion. It is worth noting that the theory of these devices is intrinsically difficult because it involves the transport of and interactions among plasmas and gases, as well as their interaction with electrode surfaces. We then give our experimental results and conclusions, including our recommendations for

an optimum gas detector.

The technical assistance of J. W. Poulton, E. S. Zavada and R. E. Hiromoto in the construction and testing of various devices is gratefully acknowledged.

II. THEORY

A. The Ionization of Gases by Radioactive Sources

The theory of the interaction between radiation and gases is discussed in many places.[2,7,15-18] The picture is simple: an alpha particle, a beta particle or a gamma ray photon incident upon a gas with sufficient energy can knock out an atomic electron from a gas atom, leaving behind a heavy, positively-charged atomic ion, and a light, negative, free electron. An interesting and useful fact about this process is that the average energy w lost by radiation in producing a single ion pair is essentially independent of the mass, charge and velocity of the bombarding particle, and depends only weakly on the nature of the gas.[2] Some typical values taken from Fulbright[2] are given in Table I, along with the ionization potential I_o.

Table I. Ionization potential I_o and average energy per ion pair w for several gases.[a]

Gas	I_o (eV)	w (eV)
Hydrogen	15.4	36.8
Helium	24.6	41.3
Nitrogen	15.5	34.9
Oxygen	12.2	31.3
Argon	15.8	26.4
Neon	21.6	35.9
Krypton	14.0	24.4
Xenon	12.1	22.1
Air	--	34.2
Carbon Dioxide	13.7	32.7
Methane	13.1	28.1

[a] Taken from Table 6 in reference 2.

That w is roughly twice as large as I_o reflects the fact that the energy lost by the bombarding radiation can be dissipated by means other than ionization, e.g., optical transitions, recoil energy, etc.

The spatial rate of energy loss by radiation has been studied theoretically and experimentally. For heavy charged particles (e.g., protons and alphas) one used the Bethe-Møller formula

$$-\frac{dE}{dx} = \frac{4\pi z^2 e^4 NZ}{mv^2}\left[\log\left(\frac{2mv^2}{I_T(1-\beta^2)}\right) - \beta^2\right], \qquad (1)$$

where

E = kinetic energy of the bombarding particle

$-\frac{dE}{dx}$ = kinetic energy loss per unit path length of the bombarding particle

ze = charge of the bombarding particle

v = velocity of the bombarding particle

e = charge of the electron

m = mass of the electron

β = v/c

c = speed of light

I_T = mean excitation energy[2,19] of target atoms

N = number of atoms of target material per cm^3

Z = atomic number of atoms in target material.

For bombarding relativistic beta particles (electrons), one uses another of Bethe's results

$$-\frac{dE}{dx} = \frac{2\pi e^4 NZ}{mv^2}\left[\log\left(\frac{mv^2 E}{2\,I_T^2(1-\beta^2)}\right) - (2(1-\beta^2)^{1/2} - 1 + \beta^2)\log 2 + (1-\beta^2) + \frac{1}{8}(1-(1-\beta^2)^{1/2})^2\right]. \qquad (2)$$

For non-relativistic ($\beta << 1$) betas, equation (2) reduces to

$$-\frac{dE}{dx} = \frac{4\pi e^4 NZ}{mv^2} \log\left(\frac{mv^2}{2I_T}\left(\frac{e'}{2}\right)^{1/2}\right) , \tag{3}$$

where e' is the base of natural logarithms.

When a bombarding particle has lost all its kinetic energy it comes to rest. The distance it has traveled in the target material in coming to rest is called the range R, and is obtained by integrating the differential energy loss of the particle in traversing the target material:

$$R = \int_0^E \frac{dE'}{\left(-\frac{dE'}{dx}\right)} . \tag{4}$$

A FORTRAN program for calculating ranges of heavy charged particles in chemical elements has been developed by Trower,[20] and some of its results are available in tabular form.[21]

If the range R of the bombarding particle is less than the interelectrode spacing d, then the number of ion pairs produced in the detector volume will be the same for all values of R regardless of variations in the gas density. However, if R > d, the number of ion pairs n_I produced by one ionizing particle will be

$$n_I = \frac{1}{w}\int_0^d \left(-\frac{dE}{dx}\right) dx . \tag{5}$$

The dependence of n_I on the density N of the detector gas is in general complicated for R > d, but is approximately linear under some circumstances. Since the detector current is a function of n_I, we see that the current varies with detector gas density only when R > d. This observation is irrelevant for glow tubes since their current does not depend on n_I.

Next we consider the relative values of n_I for alpha, beta and gamma radiation, all other parameters being held constant. As a typical example, consider a 5 MeV alpha and a 100 keV beta (both are non-relativistic). With $I_T \sim 50$ eV, we get the ratio of their $(-\frac{dE}{dx})$ values as

$$\frac{(-\frac{dE}{dx})_\alpha}{(-\frac{dE}{dx})_\beta} \sim \frac{4\,v_\beta^2}{v_\alpha^2} \quad \frac{\log \frac{2mv_\alpha^2}{I_T}}{\log \frac{mv_\beta^2}{2I_T}} \simeq 310 >> 1 \,. \qquad (6)$$

This is quite general. Because of the weak dependence of the logarithms on v_α and v_β, the ratio of (6) is dominated by the $(v_\beta/v_\alpha)^2$ term. For most radiations $v_\beta >> v_\alpha$. Thus $(-\frac{dE}{dx})$ is much greater for alphas than for betas. If we apply this result to equation (5), we see that one alpha particle will produce several orders of magnitude more ion pairs in the gas detector than a single beta particle if R > d for both particles. Conversely, to get the same number of ion pairs, one needs a beta source with an activity several orders of magnitude greater than an alpha source. It is for this reason that our ionization chamber and proportional counter detector designs utilize alpha sources only. An incidental additional advantage of alphas is that shielding problems are minimized since the range of alphas is much less than for betas.

The theory[7,15] of the interaction of gamma ray photons with matter is not straightforward as three distinct processes contribute; photoelectric effect, Compton scattering, and electron-positron pair production. We shall neglect gamma rays from consideration as a detector source because the

probability of interaction of a photon with matter is less than for a charged particle, and the resulting ratio of ion pairs produced per unit path length by photons compares unfavorably with alpha and beta particles.

It is necessary to find alpha particles which have sufficiently large ranges in gases to allow the condition R > d to be satisfied for reasonable interelectrode spacings. The range-energy relation for alpha particles in air at 15° C and 760 Torr[15] is shown in Table II. These numbers can be

Table II. Energy and range for alpha particles in air at 15° C and 760 Torr.[a]

Energy (MeV)	Range (cm)
1.0	0.52
2.0	1.01
3.0	1.67
4.0	2.50
5.0	3.51
10.0	10.52
15.0	21.50

[a] Estimated from Figure 2 in reference 15.

used with N and Z, and equations (1) and (4) to obtain approximate alpha particle ranges in other gases at various densities, if one assumes a linear dependence of $(-\frac{dE}{dx})$ on N. One notes that 5 MeV alphas have a range of over one inch in air at 15° C and 1 atmosphere. It is only necessary to check the condition R > d at the highest gas density (when the detector is filled); as the gas density decreases, R increases (see equations (1) and (4)).

A radioactive source used in an ionization chamber or proportional counter gas detector must produce particles which have 1) sufficiently high energy to satisfy the R > d condition, 2) a half-life $T_{1/2}$ long enough for adequate activity throughout the duration of the spacecraft's mission (~ 2 years), 3) a $T_{1/2}$ short enough so that one need not use great amounts or excessively large surface areas to get an adequate activity (since the probability for a radioactive decay is inversely proportional to $T_{1/2}$), 4) a daughter nucleus that is stable so that a unique activity is present (thus simplifying the analysis of the source emissions), 5) sufficiently low penetrating power so that a minimum radiation hazard exists outside the detector, and 6) availability in a form which is easy to fasten inside the gas detector. For reference purposes we have listed in Tables III and IV all alpha and beta emitters satisfying the relation (2 years) < $T_{1/2}$ < (10^4 years), since other sources will not satisfy conditions 2) and 3) above. For the ionization chamber and proportional counter designs we concentrate on alpha emitters, for the reasons given above. Availability[22] is a key factor in the choice of nuclide. A radioactive foil source is the most convenient form to fasten inside the gas detector. A readily available foil source is Americium-241,[23] which has energetic alphas (5.44 and 5.49 MeV), a 458 year half-life, and reasonable specific activities (~ 250 microcuries per cm^2). Radium-226 has gaseous decay products, a lower specific activity (since $T_{1/2}$ = 1600 years), and beta and gamma activity which is hard to shield. Gadolinium-148 and Polonium-209 have acceptable properties but are not readily available in any form. Plutonium-238 foils are not available at present, but Monsanto (Dayton, Ohio) has begun work on their production. The remaining alpha sources either are not readily available or have half-lives too long or too short. A long $T_{1/2}$ violates condition 3) because of the low specific activity.

Table III. Alpha emitters with half-lives $T_{1/2}$ between 2 and 10^4 years.[a]

Nuclide	$T_{1/2}$ (yr)	Principle or Average Alpha Energy (MeV)	Daughter	$T_{1/2}$ of Daughter	Comments[b]
Gd-148	84	3.18	Sm-144	Stable	NRA
Po-208	3	5.11	Pb-204	Stable	Short $T_{1/2}$
Po-209	103	4.88	Pb-205	3×10^7 yr	NRA
Ra-226	1600	4.78	Rn-222	3.8 days	See Text
Th-228	1.9	5.4	Ra-224	3.64 days	Short $T_{1/2}$
Pu-236	2.85	5.76	U-232	72 yr	Short $T_{1/2}$
Pu-238	86.4	5.49	U-234	2.5×10^5 yr	See Text
Pu-240	6580	5.16	U-236	2.4×10^7 yr	Long $T_{1/2}$
Am-241	458	5.48	Np-237	2×10^6 yr	See Text
Am-242m	152	5.21	Np-238	2.1 days	NRA
Am-243	8000	5.27	Np-239	2.35 days	NRA
Cm-243	32	5.79	Pu-239	2.4×10^4 yr	NRA
Cm-244	17.6	5.8	Pu-240	6580 yr	NRA
Cm-245	9300	5.35	Pu-241	13.2 yr	NRA
Cm-246	5500	5.38	Pu-242	3.8×10^5 yr	NRA
Cf-249	360	5.81	Cm-245	9300 yr	NRA
Cf-250	13.2	6.02	Cm-246	5500 yr	NRA
Cf-251	800	5.85	Cm-247	1.6×10^7 yr	NRA

[a] Data taken from C. M. Lederer, J. M. Hollander and I. Perlman, Table of Isotopes, Sixth Edition (John Wiley & Sons, New York, 1967).

[b] NRA = Not readily available.

Table IV. Beta emitters with half-lives $T_{1/2}$ between 2 and 10^4 years.[a]

Nuclide	$T_{1/2}$ (yr)	Maximum Beta Energy (MeV)	Daughter	$T_{1/2}$ of Daughter
H-3	12.3	0.0186	He-3	Stable
C-14	5730	0.156	N-14	Stable
Na-22	2.6	1.82	Ne-22	Stable
Si-32	650	0.21	P-32	14.3 days
A-39	269	0.565	K-39	Stable
A-42	33	(3.52 from K-42)	K-42	12.4 hr
Co-60	5.3	0.313	Ni-60	Stable
Ni-63	92	0.067	Cu-63	Stable
Kr-85	10.76	0.67	Rb-85	Stable
Sr-90	28	0.546	Y-90	64 hr
Ru-106	1	0.039(3.54 from Rh-106)	Rh-106	30 sec
Cd-113m	14	0.580	In-113	Stable
Sn-121m	76	0.420	Sb-121	Stable
Sb-125	2.7	0.61	Te-125m	58 days
Cs-134	2	0.662	Ba-134	Stable
Cs-137	30	1.176	Ba-137m	2.55 min
Pm-147	2.6	0.224	Sm-147	Stable
Eu-154	16	1.85	Gd-154	Stable
Eu-155	1.8	0.25	Gd-155	Stable
Ho-166m	1200	0.07	Er-166	Stable
Tm-171	1.9	0.097	Yb-171 (Yb-171m)	Stable (8 days)
Os-194	6	0.053	Ir-194m	47 sec
Tl-204	3.8	0.766	Pb-204	Stable

Table IV. Cont.:

Nuclide	$T_{1/2}$ (yr)	Maximum Beta Energy (MeV)	Daughter	$T_{1/2}$ of Daughter
Pb-210	21	0.061	Bi-210	5 days
Ra-228	6.7	0.05	Ac-228	6.13 hr
Ac-227	22	0.046	Th-227	18.2 days
Pu-241	13.2	0.021	Am-241	458 yr

[a] Data taken from C. M. Lederer, J. M. Hollander and I. Perlman, Table of Isotopes, Sixth Edition (John Wiley & Sons, New York, 1967).

We have considered the feasibility of using Argon-39 or Krypton-85 as a combined beta source - detector gas for the ionization chamber and proportional counter. While the radiation hazard is not negligible, this presents an amusing solution to the problem of mounting the radioactive source in the detector. We calculate that 1 cm^3 of A-39 (Kr-85) at standard temperature and pressure has an activity of 60 millicuries (1.5 curies). These activities are roughly equivalent to a 200 microcurie (5 millicurie) alpha source (see equation (6)), respectively, in terms of ion pair production.

Finally, we consider the radioactive source requirements for a glow tube. Radiation in some form (light, radioactivity) is necessary for the most effective firing of a glow tube, but is not needed to sustain the current once breakdown has occurred. Because the detector is light tight, a weak radioactive source is helpful in firing the tube, but one need not worry about the $R > d$ condition. One possibility is to add a small amount ($\sim$ 1 μCi) of A-39 or Kr-85 to the glow tube gas. Alternatively, one could solder into the detector a small piece ($\sim$ 1 μCi) of radioactive metal, for example, Cobalt-60. If nickel electrodes are used, they can be irradiated with thermal neutrons to activate Ni-63, a beta emitter.

B. Ionization Chambers

The ionization chamber[2-7] is a low current - low voltage device which can be used for detecting radiation - produced ionization in gases, and has been utilized in commercial radioactive ionization pressure gauges. The usual configuration is the parallel plate geometry, as shown in Figure 3. The guard ring serves two functions: it makes the electric field between the two electrodes more homogeneous by minimizing edge effects, and allows one to ignore leakage currents through the insulators. The theory of the dynamics

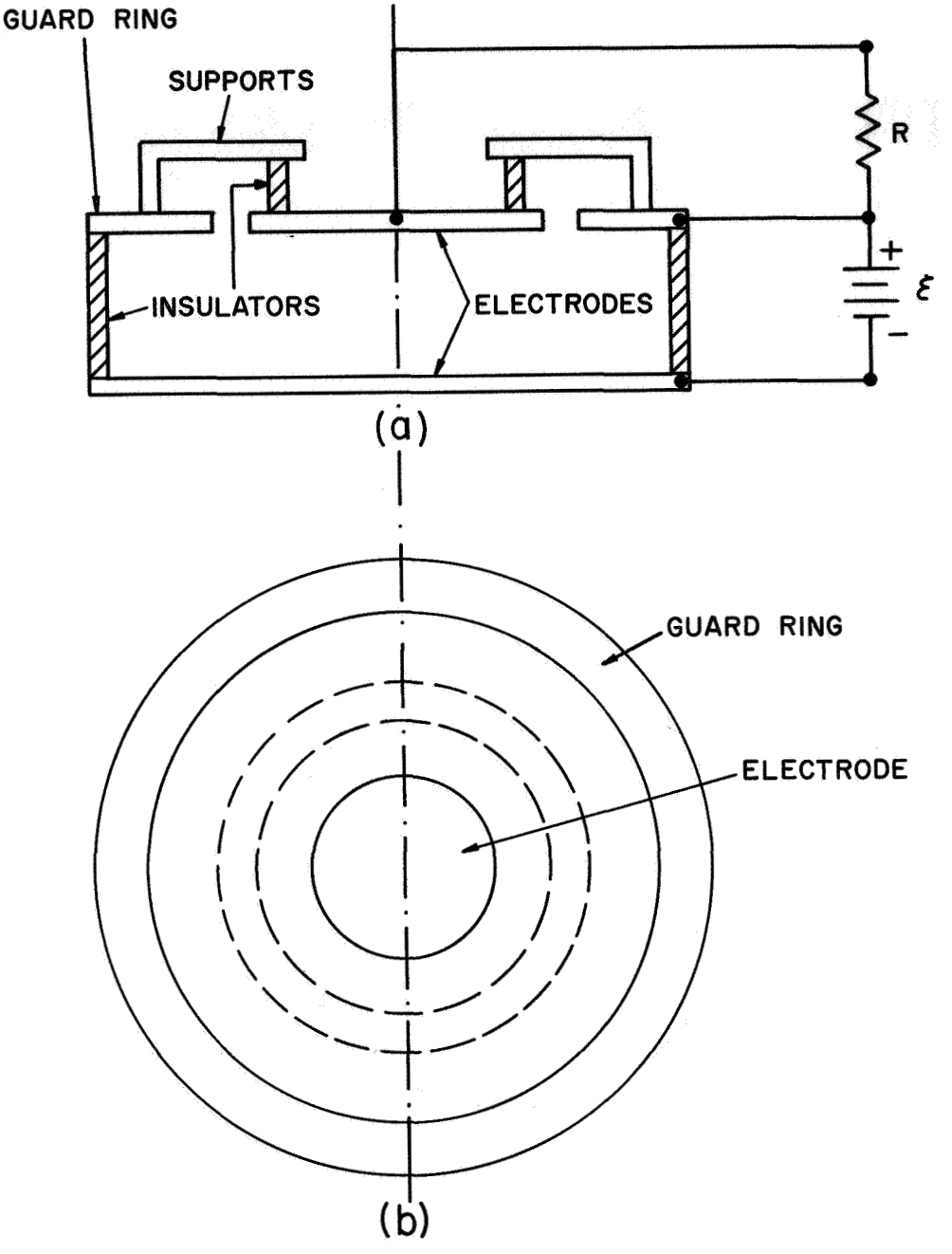

Figure 3. Typical parallel plate ionization chamber. (a) Side view and schematic. (b) Top view.

of the ion and gas movements in this device is very complicated. We summarize the main processes below.

Recombination is the process whereby a positive ion and an electron collide to form a neutral atom. The rate of recombination is given by

$$\frac{dn_e}{dt} = \frac{dn_+}{dt} = -\alpha n_+ n_e \quad , \tag{7}$$

where n_+ and n_e are the number of positive ions and electrons, respectively, per unit volume, and α is the coefficient of recombination. Since n_+ and n_e are both proportional to n_I in ionization chambers, we see that

$$\frac{dn_e}{dt} = \frac{dn_+}{dt} \propto N^2 \quad , \tag{8}$$

if n_I is a linear function of the gas density N. Thus recombination becomes more of a problem as the gas density increases. Ions which recombine do not contribute to the detector current. One usually speaks of three kinds of recombination processes: 1) volume recombination (throughout the interelectrode sensitive volume), 2) columnar recombination (along the track of the bombarding particle), and 3) preferential recombination (of slow electrons near the positive ion from which they were originally detached). Discussion of recombination mechanisms and typical values are given in the references.(2-7)

Electron attachment refers to the capture of an electron by a neutral molecule to form a negative ion. It is a large effect in O_2, H_2O, NH_3, HCl, SiF_4 and the halogens, and is negligible in N_2, H_2, CO_2, CH_4 and the rare gases. This process effectively changes the mass of a negative ion from very light (electron) to very heavy (molecule with attached electron). Now the current density J_- of the negative ions is given by

$$J_- = n_- e v_- \quad , \tag{9}$$

where v_- is the drift velocity of the negative ions. In the same electric field, a heavy ion has a much smaller drift velocity than does an electron. Hence electron attachment tends to decrease the detector current.

Let us now consider the behavior of the atomic ions after their creation. The atomic ions thermalize locally (in space) with a temperature close to that of the neutral gas atoms of the detector. Superimposed on their fast random thermal motions is a slow drift velocity toward one of the electrodes (e.g., the positive ions toward the cathode). One finds experimentally for this diffusion of ions that

$$\vec{v}_{\pm} = \mu_{\pm} \frac{\vec{E}}{P} \quad , \tag{10}$$

where $\vec{v}_{\pm}$ is the drift velocity (<< thermal velocity) of the positive and negative atomic ions, respectively, $\mu_{\pm}$ is their mobility, $\vec{E}$ is the applied electric field, and P is the gas pressure at normal temperature (0° C). Ionic mobility depends on the charge and mass of the ion and on the nature of the host gas, and typical values are given in the references.[2-7]

The behavior of the free electrons is slightly more complicated. Because of the small electron-to-ion mass ratio, electrons cannot lose much kinetic energy in elastic collisions with the much heavier gas atoms, and hence only lose energy in inelastic collisions in which they excite the gas atoms. The energies of the lowest-lying excited states of monatomic (i.e., rare) gas atoms are typically ~ 10 eV above their ground states. Thus the free electrons quickly attain an average "agitation energy" of 10 eV for their random thermal motions, since electrons of greater energy rapidly excite the gas atoms. The electric field $\vec{E}$ accelerates the electrons up to 10 eV. We do not call this a "thermal energy" because the velocity distribution is usually not Maxwellian. We note that the electrons are

much "hotter" than the atomic ions or gas molecules (kT ≈ .025 eV at room temperature).

Superimposed upon the agitation motion of the electrons is their diffusion toward the anode with a drift velocity $\vec{v}_e$ << rms agitation velocity u. Typically

$$\vec{v}_e \sim 10^3 \vec{v}_{\pm} \quad , \tag{11}$$

so that the electrons drift much faster than the atomic ions, as expected. We get more insight by recalling the simple theory of drift velocity[3,24] which gives

$$\vec{v}_e = \frac{e\tau}{m} \vec{E} \quad , \tag{12}$$

where τ is the mean free time between collisions. The assumptions in this crude theory are that all the electrons have the same agitation energy $E_a = 1/2\ m\ u^2$, and that the scattering is isotropic. We can write the mean free path λ as

$$\lambda = u\tau \quad . \tag{13}$$

Thus

$$\vec{v}_e = \frac{e\lambda}{mu} \vec{E} = \frac{e\lambda}{(2mE_a)^{1/2}} \vec{E} \quad . \tag{14}$$

Hence a large agitation energy E_a leads to a low drift velocity. One can decrease E_a, and thus increase $\vec{v}_e$, in rare gas detectors by adding a few percent N_2, CO_2, CH_4, or some other polyatomic gas. The latter have excited rotational and vibrational states ~ 1 eV above their ground state, so that the agitation energy of the electrons is reduced by a factor of roughly ten.

This increases the mean free path λ, too. Because of a quantum mechanical phenomenon called the Ramsauer effect,[2,25] the total cross section for the scattering of electrons by rare gas atoms has a minimum at about 1 eV incident electron kinetic energy.

The addition of a small polyatomic impurity such as CO_2 or CH_4 to a rare gas reduces the electron attachment to any minute O_2 impurities present.[2] The probability for this latter process has a minimum for electrons of energy 1 eV. It has been found experimentally[2] that 0.1% O_2 in pure argon leads to significant electron attachment, but that the addition of 2% CO_2 (or CH_4 or N_2) to this mixture reduces the attachment.

Consider now the operation of a direct current (dc) ionization chamber in the presence of a source of constant activity. Fast pulse ionization chambers and proportional counters are more useful in nuclear physics for detecting individual radiations. Recall that in the ionization chamber region, the ion pairs in the gas are produced only by the bombarding radiation; there is no multiplication. The current versus voltage curve for a typical chamber at fixed gas density is shown in Figure 2, O to B. From O to A, not all the ion pairs are collected by the electrodes; $\vec{v}_e$ is small due to the small $\vec{E}$ (= V/d in a parallel plate device), and many of the ions recombine before reaching the electrode. Others diffuse out of the "sensitive region" of the chamber and are not collected. The segment A to B is called the saturation region. Here all the ion pairs are collected by the electrodes, as $\vec{v}_e$ is large enough so that recombination is negligible. Space charge effects in parallel plate ionization chambers are often negligible, although we have calculated[3] significant space charges for some of our experimental conditions.

The expected current is easily estimated. If we have an alpha source with an effective activity of 1 mCi (= 3.7×10^7 disintegrations per second) and an alpha energy of 5 MeV, assume that 2.5 MeV is lost on the average by each alpha particle in the chamber, and take a w value of 30 eV, then the number of ion pairs produced per second is

$$\dot{n}_I = \frac{(2.5 \times 10^6 \text{ eV})(3.7 \times 10^7 \text{ sec}^{-1})}{30 \text{ eV}} \sim 3 \times 10^{12} \text{ sec}^{-1} . \quad (15)$$

Each ion pair contributes e in electric charge to the current.[3] In the steady state of dc operation at saturation, all the ion pairs produced by the radiation in one second are collected by the electrodes in the same time period. Hence, the current I through the chamber will be

$$I = e \dot{n}_I \sim 4.8 \times 10^{-7} \text{ A} . \quad (16)$$

Note in Table I that all gases have the same w value (~ 30 eV) within about 30 - 40%. Our conclusion is that all gases will have the same order of magnitude saturation current in a dc ionization chamber with a given constant activity source at a given filling pressure. Furthermore, for reasonable alpha sources (5 MeV energy with < 1 mCi activity), the currents will typically be less than 10^{-6} A. Actually, it is difficult to find small alpha sources with activities of 1 mCi, and we shall see that a current ~ 3×10^{-7} A is our experimental maximum. These currents are difficult to detect under the constraints of flight conditions.

We have considered the possibility of increasing these small currents by operating in an alternating current (ac) mode. Perhaps, we thought, the small ac currents could be amplified, and the amplified output could then (hopefully) be proportional to the gas density. If the chamber is

represented as an interelectrode capacitance C in parallel with a large leakage resistance R_L (the ionized gas), the capacitive reactance $X_C \ll R_L$ for any reasonable parallel plate or coaxial geometry at low audio frequencies. Thus the net impedance of the chamber is entirely determined by X_C, and the ac current would be insensitive to changes in R_L.

Figure 4 shows a rough plot of the gas density dependence (pressure dependence if the temperature is fixed) of the ionization chamber current at fixed voltage. The dependence is approximately linear except at the extremes. At high densities, the curve bends over if the electric field $\vec{E}$ is not sufficiently large to avoid recombination losses, whereas at very low gas densities there is a residual current $\sim 10^{-12}$ A.[6] The latter is not conducted via the gas, but is due to electrons and other ions produced at the walls and electrodes by the ionizing particles.

C. Proportional Counters

Many of the ideas of the last section apply equally well to proportional counters[3-5,7-9], and we indicate here only the new features. Proportional counters are usually designed with a coaxial geometry, to take advantage of the large fields near the central electrode. The electric field magnitude E_r at a distance r from the axis of the counter is

$$E_r = \frac{V}{\ln\left(\frac{b}{a}\right)} \frac{1}{r} , \qquad (17)$$

where a is the outside radius of the inner conductor wire, b is the inner radius of the outside cylindrical conductor, and V is the voltage across the counter. Cylindrical guard rings are often used with this geometry. Close to the center electrode wire, which is maintained at a positive polarity, the electric field E_r becomes large, and electrons produced by the ionizing

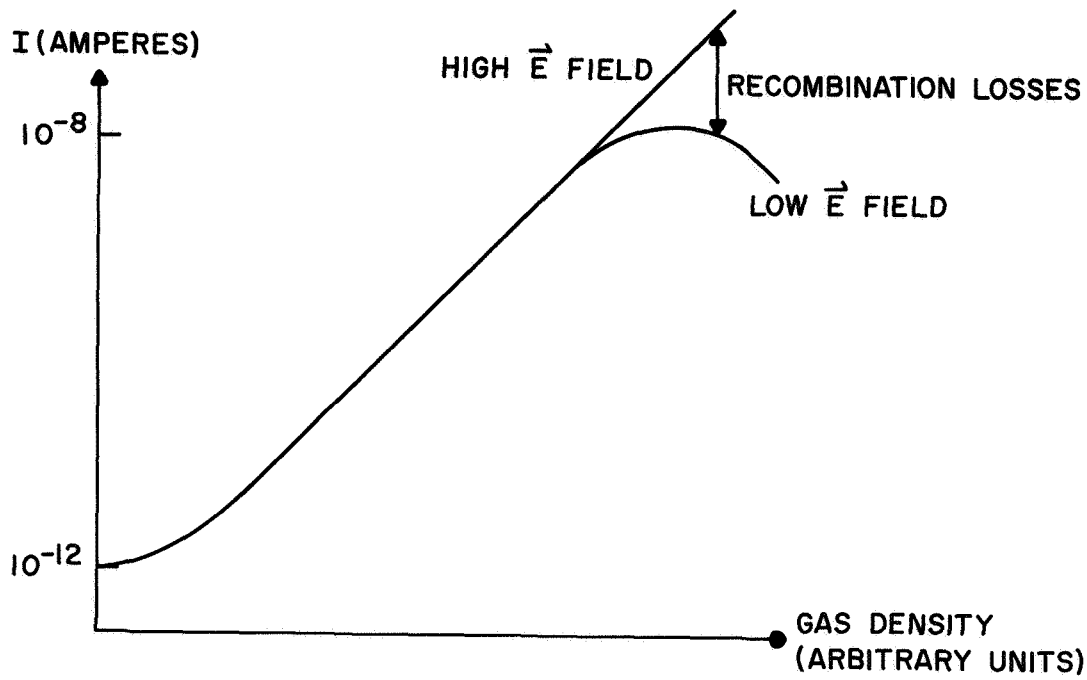

Figure 4. Typical gas density dependence of ionization chamber current at fixed voltage.

radiation can themselves attain sufficient energy between collisions to ionize additional gas molecules and thus produce more electrons. Let us relate the average total number of secondary electrons n produced by a single primary electron to the multiplication factor M. Recall that many photons are given off in the avalanche process, and that these photons can eject electrons from the walls of the container and from the gas molecules. If γ ($<< 1$) is the average number of photoelectrons produced by one ion pair in the gas, then the initial avalanche due to one primary electron produces $n\gamma$ photoelectrons, and the latter multiply by the factor n before collection at the anode to give a total of $n^2\gamma$ electrons. The latter produce $n^2\gamma^2$ photoelectrons which multiply by n to give $n^3\gamma^2$ total electrons before collection, and so on. Hence the total multiplication M is

$$M = n + n^2\gamma + n^3\gamma^2 + \ldots\ldots , \tag{18}$$

or

$$M = \frac{n}{1 - n\gamma} , \tag{19}$$

if $n\gamma < 1$. In the limit $n\gamma << 1$, equation (19) becomes

$$M \simeq n . \tag{20}$$

Equation (20) is the condition for a "proportional" counter in that the output current of the counter is proportional to the number of primary electrons produced by the ionizing radiation if photoelectron production is negligible. In the above treatment we are ignoring recombination and electron attachment losses. Space charge effects are often negligible. For large electric fields, small ionizing radiation activity, and n not too large, these are valid approximations.

As $n\gamma$ approaches unity, the counter becomes non-proportional, and the multiplication very large. At $n\gamma = 1$ the multiplication is infinite, telling us that a self-maintaining discharge would be set up (e.g., Geiger-Muller counter, glow tube, etc.). This depends not only on the gas (n variation) but also on the photoelectric properties of the electrodes (γ variation). Values of M up to 10^4 can be obtained, but operation becomes unstable when $n\gamma \to 1$, i.e., when n is large.

The current-voltage characteristics of a typical proportional counter in the dc mode with fixed gas density and constant radiation activity are shown in Figure 2, B to C. The current is given by

$$I = e \dot{n}_I M \quad . \tag{21}$$

A simple theory in fairly good agreement with experiment[4] gives

$$M = \exp\left[k \left(\frac{V}{(aP) \ln(\frac{b}{a})} \right)^{1/2} \left(\left(\frac{V}{k' (aP) \ln(\frac{b}{a})} \right)^{1/2} - 1 \right) \right] , \tag{22}$$

where k and k' are constants for a given gas, and P is the pressure at fixed temperature. If $V >> k'(aP)\ln(\frac{b}{a})$ (= threshold voltage for multiplication), then we get

$$I = e \dot{n}_I \exp\left[\frac{k}{\sqrt{k'} \ln(\frac{b}{a})} V \right] . \tag{23}$$

Hence I is an exponential function of V and is approximately proportional to the gas density through the $\dot{n}_I$ factor. Neither dependence is true for lower voltages. Furthermore, at low gas densities ($\sim$ 1 torr at room temperature) where the mean free path of the electrons becomes large, n becomes large, and M changes rapidly with variations in both V and the gas density. We would expect the addition of a small amount of CO_2 or CH_4 to a

rare gas in the counter to smooth out these rapid variations by lowering the electronic agitation energy.

Since multiplications of 10^2 to 10^3 are reasonable in proportional counters and since typical ionization chamber currents go up to 10^{-7} A, proportional counters should give currents up to 10^{-5} or 10^{-4} A at voltages $\gtrsim$ 1000 V. We shall see many of the features of this discussion in our experimental results.

D. Glow Tubes

Cold cathode glow tubes[10-14] are usually constructed with a coaxial geometry or else with two parallel conducting rods enclosed in a glass container. The device typically has a low current (<< 1 mA) due to residual ionization at low voltages, and then "breaks down" to give currents ~ 1 mA at some voltage V_s called, variously, the striking, breakdown, firing, sparking, ignition, or starting voltage. The tube is usually operated in the normal glow discharge region (E to F in Figure 2) at a running (or maintaining) voltage V_r, with $V_s \gtrsim V_r$. Glow tubes are self-maintaining in that they will continue to run at normal glow even if the cause of the residual ionization (which is necessary for breakdown) is removed after the tube has been fired. Cosmic rays are a natural contributor to the residual ionization. External light and radioactive sources are much more effective, and many manufacturers add a small amount (~ 1 μCi) of H-3 or Kr-85 to commercial glow tubes so that their characteristics will not change too much if they are operated in the dark.

If a device is to be self-maintaining in the normal glow region, it must produce new ion pairs in the gas to replace those that are collected at the

electrodes. The chief mechanism is one that is usually negligible in the proportional counter regime. When the positive ions reach the cathode and neutralize by combining with an electron, there is a finite probability that one or more extra electrons will be ejected from the cathode surface to contribute to the electron avalanche and interelectrode current. This process of electron production by positive ion bombardment depends on the properties of the cathode material and surface as well as those of the gas, and is usually stronger than photoelectron production.

The theory of glow tubes is very involved and we discuss here only a few points which help in understanding their design and operation. A first characteristic is that glow tubes always have a large space charge. In fact, most of the voltage drop across a tube in the normal glow discharge regime occurs in a small region near the cathode occupied by a relatively large number of positive ions and only a few electrons. This region of the "cathode fall" is where most of the glow of the tube occurs. The rest of the interelectrode spacing, called the plasma, has roughly equal numbers of positive atomic ions and electrons.

A second feature is that the current density J (current per unit area of the cathode) in the normal glow discharge region is approximately a constant. Thus, as one goes from E to F in Figure 2, the amount of glow spreads from a small part of the cathode (at E) until the entire length of the cathode is glowing (at F). The glowing region along the cathode has fixed current density, while the unglowing part has negligible current. Thus the area of the cathode covered by the glow is proportional to the total current I through the tube. One can show[10] that

$$J \propto (\text{gas density})^2 \quad . \tag{24}$$

An approximate rule with considerable theoretical and experimental validity is Paschen's Law, which states that at fixed temperature and with parallel plates, the breakdown voltage V_s is a function of the product of the pressure P and distance d between the two parallel electrodes:

$$V_s = f(Pd) \quad . \tag{25}$$

The function f depends on the gas and on the cathode material and surface. For variable temperatures, one reads "gas density" for P. One can deduce related results for other geometries. In a fixed geometry the breakdown voltage V_s is expected theoretically to be large at both high and low gas densities, and to pass through a minimum in between. Qualitatively this is obvious. At high densities the electron mean free path is short, so that it does not acquire much energy between collisions, and thus does not usually possess sufficient energy to ionize gas atoms and produce an electron avalanche. There are not many gas atoms available at low densities, so that an electron avalanche is not probable.

One can reduce V_s and V_r through the use of Penning mixtures such as 99 1/2% Ne - 1/2% A (or 99 1/2% He - 1/2% A). During the electron avalanche, the neon atoms, in addition being ionized, are excited to metastable states (Ne*) which have a long lifetime ($\sim 10^{-2} - 10^{-4}$ sec) compared to the mean time between atomic collisions ($\sim 10^{-10}$ sec) or the mean lifetime for radiative de-excitation ($\sim 10^{-7} - 10^{-10}$ sec). The energy of Ne* is 16.6 eV (relative to its ground state), while the ionization energy I_o of argon is 15.8 eV. Thus an energetically allowed reaction is

$$Ne^* + A \rightarrow Ne + A^+ + e^- \quad . \tag{26}$$

The Ne* can produce an argon ion A^+ and an electron e^-. Hence neon metastable states can be turned into argon ions and electrons, thus enhancing the

ionization of the system as compared with pure neon gas. The effect is observed in the He - A mixture (since He* is 19.8 eV) and other mixtures. The only necessary requirement is that the host gas metastable state have a higher energy than the impurity gas ionization energy, while the more nearly equal the two energies, the more probable it is that the transfer reaction occur. The largest effect is for Ne - A and He - A, and they are thus the most commonly used. The effect of the increased ionization is to lower the striking voltage V_s and the running voltage V_r, an effect which is most pronounced in the Ne-A mixture. One observes a minimum in V_s and V_r with argon admixtures between 0.1 and 1.0% in a neon glow tube. At lower admixtures there are insufficient argon atoms, and at admixtures higher than 1%, electrons begin to ionize argon directly so that the tube behaves more like an argon device.

A few words about the effect of the cathode material and surface are in order. Early workers in this field found that the breakdown voltage V_s for a given gas at a given pressure was independent of the cathode material.[11] Later work showed that these results were caused by "dirty" cathode surfaces, e.g., oxides, adsorbed gases, etc. With modern outgassing techniques in high vacuums, one can obtain clean surfaces and see the dependence of V_s and V_r on the cathode materials. Acton and Swift[10] give the measured values of the minimum running voltage V_r^{min} for 99 1/2% Ne - 1/2% A mixtures with various cathode materials: $BaCO_3$ (55 V), evaporated potassium (62 V), evaporated magnesium (79 V), sputtered molybdenum (84 V), sputtered nickel (113 V) and unsputtered nickel (136 V). The results for 99 1/2 % He - 1/2% A are roughly 20% higher for each material. The minimum striking voltage V_s^{min} is about 20 volts higher than V_r^{min}. Of course, V_s^{min} and V_r^{min} occur at a

particular value of (Pd) for a given gas and cathode. It is important to emphasize that high purity gases and careful construction and outgassing techniques must be used in order to obtain stable, optimum performance. It should also be mentioned that the dependence of V_r and V_s on the cathode material is not as noticeable at high gas densities (Pd > 500 Torr-cm at room temperature).[10]

A process of considerable importance is sputtering. The positive ions bombarding the cathode can eject atoms as well as electrons, tending to destroy the cathode and deposit cathode material on the walls of the device. A crude empirical rule predicts that the rate of sputtering is very roughly proportional to the inverse fifth power of the gas density. The sputtered atoms also tend to absorb gas molecules (even the rare gases, although at a slower rate than other gases) on their way from the cathode to the walls, and thus to reduce the gas density and speed up the rate of sputtering. This runaway process will eventually destroy the tube. If the sputtering rate is low, however, then these processes will be beneficial because they will clean off the cathode surface and preferentially absorb impurities in a rare gas glow tube. Many commercial glow tubes are "pre-aged" by running them 24 hours in the abnormal glow discharge region (F to G in Figure 2) at twice their rated normal glow current density J, and then 24 hours at the rated normal glow current density.[10,14] With the cathodes and gases cleaned up by this "pre-aging", the tubes are supposed to have more stable characteristics in operation. It is worth noting that aluminum, magnesium and barium do not sputter as readily as do molybdenum, tantalum, nickel, copper and silver.

III. EXPERIMENTAL PROCEDURE

A schematic diagram of the experimental apparatus is shown in Figure 5. The apparatus was all standard. The voltmeters used were either a vacuum tube voltmeter (VTVM) or a regular Simpson Meter (VOM) when high input impedance was not required. Current was measured with an electrometer (range 10^{-12} to 10^{-1} A). The resistor R was zero for the ionization chamber and proportional counter experiments, and was adjustable at non-zero values for the glow tube work. Both homemade and commercial power supplies were used to provide a variable emf ε from 0 to 5000 V. The vacuum arrangement in Figure 5 is the final design used in the later stages of our work; the oil diffusion pump and Phillips gauge were not utilized in much of the earlier experimentation. All voltage measurements reported here are accurate to $\pm$ 10%, the current accuracy is $\pm$ 5%, and the pressure measurement accuracy is $\pm$ 0.1%.

Several vacuum chambers of various designs were used in the course of this work. For the parallel plate electrode configurations, provisions were made to vary the distance between the plates as well as to interchange plates of different cross-sectional area. Circular brass electrodes were utilized for the parallel plate geometry. A radioactive foil was fastened to such an electrode by sandwiching it between the flat side of the plate and a thin ($\sim$ 1/16 in.) annular brass piece (cutout area $\lesssim$ area of the foil). The latter was fastened to the electrode with two small flathead brass screws through countersunk holes in the annulus.

A typical coaxial proportional counter consisted of a copper wire central electrode along the axis of a brass tube, the wire being supported at each end of the tube by a glass-to-metal seal with a tubular inner

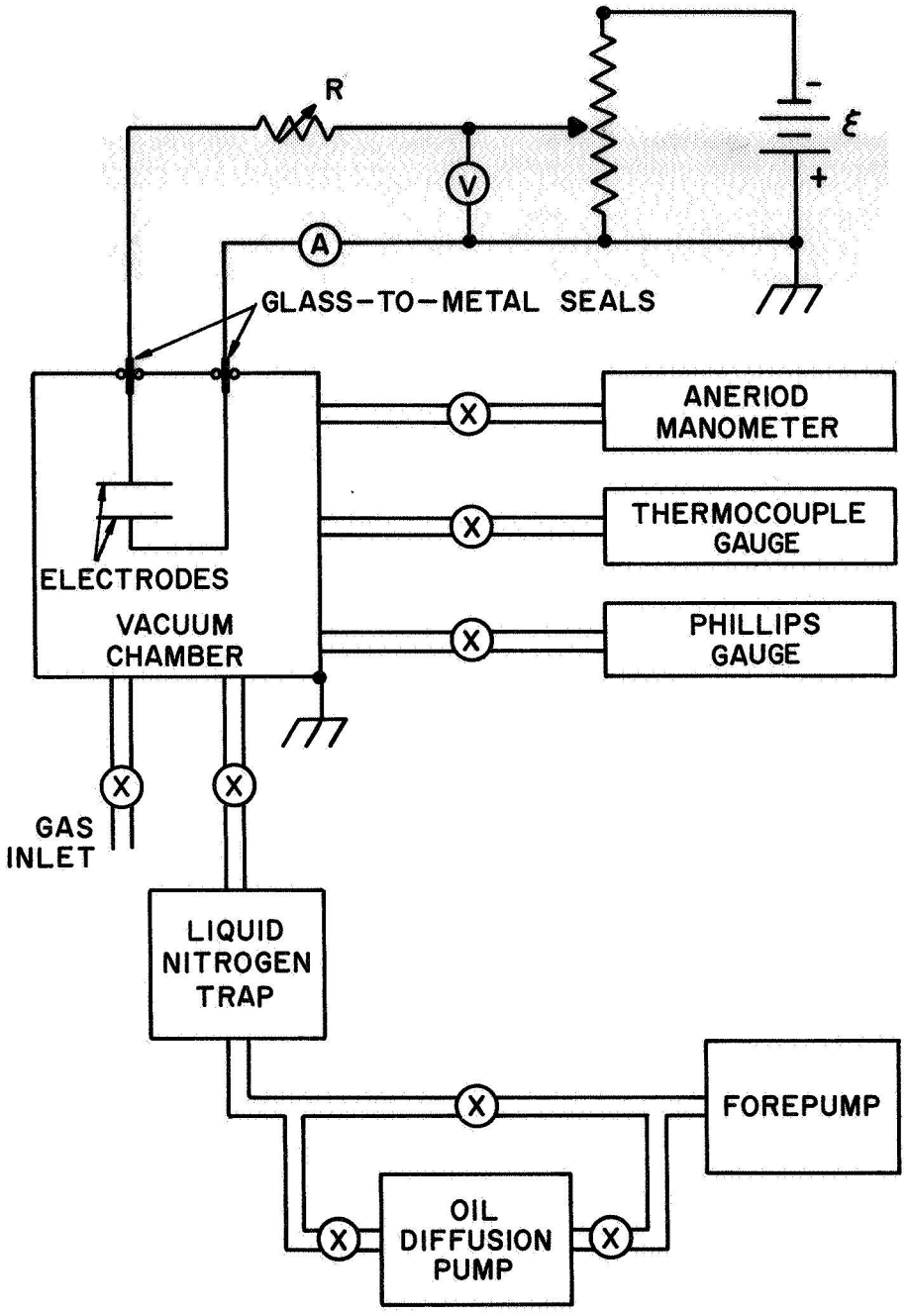

Figure 5. Schematic diagram of the experimental apparatus.

conductor (to which the wire was soldered). A radioactive foil was bent and held in place against the inside wall of the outer conductor by a small wire spring clip.

Two kinds of glow tube electrodes were utilized. Commercial neon glow lamps were stripped down to their two parallel cylindrical electrodes (barium-strontium surfaces). In addition, homemade coaxial devices similar to the proportional counter design (except without the radioactive foil) were constructed. We observed that even a VTVM loaded the glow tubes when inserted directly across the tube electrodes. Hence the VTVM was located as shown in Figure 5, and the voltage across the tube was computed by subtracting the potential drop across the resistor R from the VTVM reading. The drop across the ammeter is negligible, of course.

In all our experiments, the vacuum chamber was first pumped out and flushed several times, and then was filled with gas to the highest pressure to be tested. Lower pressures were obtained by pumping on the system. In the case of gas mixtures, the main constituent was used for flushing. After flushing, the impurity gas was admitted to the chamber first to a low pressure, and then the main constituent gas was admitted to a high pressure, the ratio of the two pressures giving the relative percentages of the two gases. This order is necessary to obtain a rapid mixing of the two gases.

IV. EXPERIMENTAL RESULTS

A. Ionization Chambers

Parallel plate ionization chambers were tested by varying the gas, gas density, voltage, radioactive source activity, electrode area, and distance between the electrodes. Considerable data with circular brass electrodes were taken at room temperature and we compress them here to give the main results. Four Americium-241 alpha foil sources from Radiation Materials Corporation (124 Calvary Street, Waltham, Massachusetts) were utilized: 1 Model AF.2 (100 μCi nominal activity, .8 in. x .25 in.), 1 Model AF.3 (250 μCi nominal activity, .8 in. x .5 in.), and 2 custom foils (each 1000 μCi nominal activity, 4.2 cm x 2.0 cm).

Figure 6 shows ionization current data taken for a 90% argon – 10% helium mixture as a function of applied voltage V at three pressures. Note that the onset of saturation occurs at higher voltages as the pressure goes up (see equation (8)). Current I as a function of gas pressure is shown in Figure 7 for the A-He mixture at 175 V under otherwise identical conditions. The curve is linear in the middle and begins to bend over slightly at higher pressures due to the onset of recombination. Also plotted in Figure 7 are data for air under identical conditions. This illustrates dramatically that the dc operation of these chambers is quite insensitive to the gas used. Further evidence of this is shown in Tables V and VI. The saturation current I_{SAT} is the constant value of I for saturation of the ionization chamber at a given pressure, and the saturation voltage V_{SAT} is defined as the lowest voltage at which the chamber is still saturated at a given pressure. Examination of Tables V and VI indicates that all the gases and gas mixtures have identical

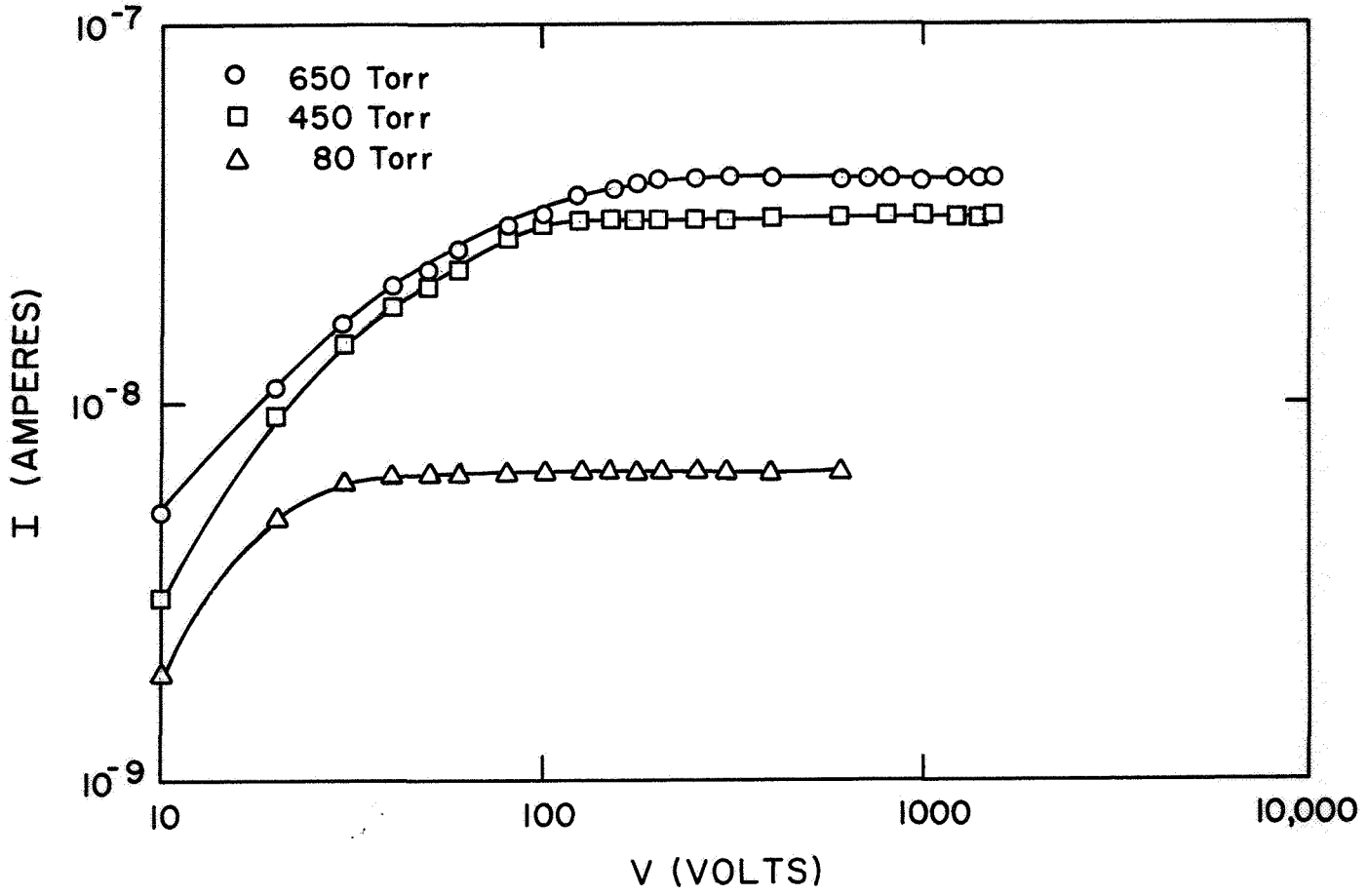

Figure 6. Ionization current I versus voltage V for 90% argon - 10% helium at room temperature. Configuration was two circular parallel plate electrodes (each 1 in. in diameter) spaced 5/16 in. apart. Source was a single 250 μCi Am-241 foil mounted on one electrode.

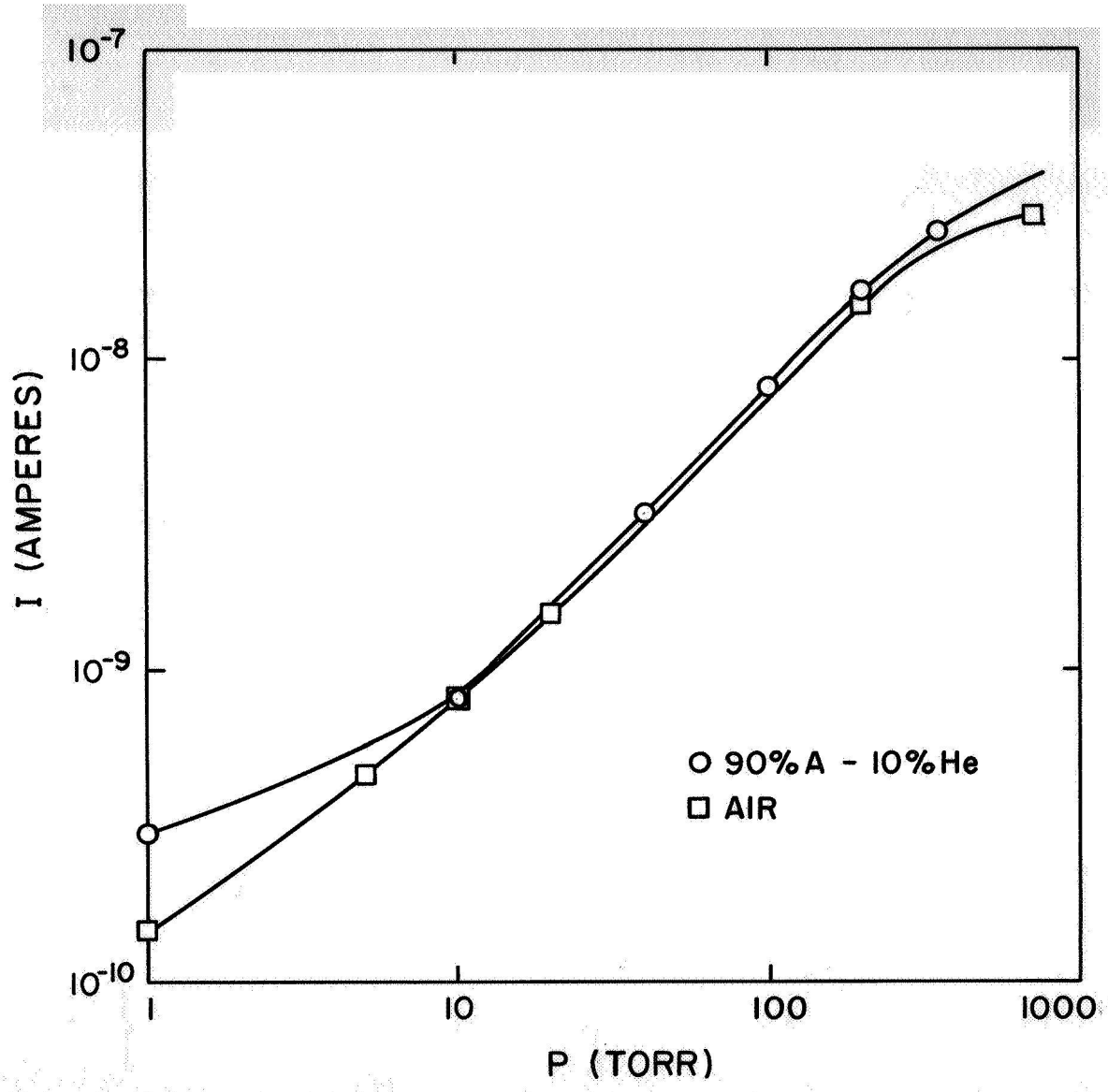

Figure 7. Ionization current I versus pressure P at 175 V and room temperature for 90% argon - 10% helium and air. Same configuration as in Figure 6.

Table V. Saturation current I_{SAT} and saturation voltage V_{SAT} at three different pressures using the same configuration as in Figure 6.

Gas	650 Torr		450 Torr		80 Torr	
	I_{SAT} (10^{-9} A)	V_{SAT} (V)	I_{SAT} (10^{-9} A)	V_{SAT} (V)	I_{SAT} (10^{-9} A)	V_{SAT} (V)
Pure A	40.5	250	34	250	7.3	125
90% A - 10% CH_4	40	200	34	180	7.4	125
90% A - 10% CO_2	40.5	250	34	150	7.5	80
90% A - 10% He	39	250	31	150	6.5	125
Pure He	10.2	100	7.3	50	1.5	40

Table VI. Ionization current I at two pressures using the same configuration as in Figure 6 at 175 V.

Gas	I (10^{-9} A) at 700 Torr	I (10^{-9} A) at 1 Torr
Pure A	41	0.22
90% A - 10% CH_4	40	~ 0.1
90% A - 10% CO_2	40	0.28
90% A - 10% He	38.5	0.3
Pure He	10.8	0.15
Air	28	0.15
Pure N_2	~ 30	—
Pure H_2	~ 10	—
Pure CH_4	~ 40	—

characteristics within a factor of 4 under otherwise identical conditions.

Numerous variations on the above conditions were made. We measured the same current with and without a guard ring under otherwise identical conditions, and therefore discarded this as an unnecessary feature. Variation of the diameter of the electrode plates and the interelectrode spacing d produced no dramatic results. In fact, if the electric field (= V/d) is kept constant, the only effect of changing the diameter and the spacing d should be to change the total number of ion pairs n_I produced by the radiation. We expect n_I, and thus I, to be approximately proportional to the volume of gas between the two electrodes. Our measurements were in rough agreement with this prediction. Finally, the variation of current with different Am-241 source activities was studied. Because of the nominal character of the rated activities and the different areas of the various foils, it was not convenient to get highly accurate data on the activity dependence of I. Crude interpolations gave the current as roughly proportional to the activity, but we claim no great accuracy for this result.

We made an attempt to see how large a current we could get with two high activity (1000 μCi each) Am-241 foils and large electrode area (one plate had 2 7/8 in. diameter, the other, 3 3/8 in. diameter). One foil was attached to each electrode, with the two foils facing each other. Although this geometry is too large for convenient use on a spacecraft, we made the test to check the maximum current obtainable under relatively optimum conditions. The results for pure argon are shown in Figure 8. At 1 atmosphere pressure the maximum current obtained was 2.8×10^{-7} A at 300 V with a 1 in. spacing. This is roughly a factor of 2 lower than the current given in equation (16), and shows the practical upper limit for this type of device with moderate source

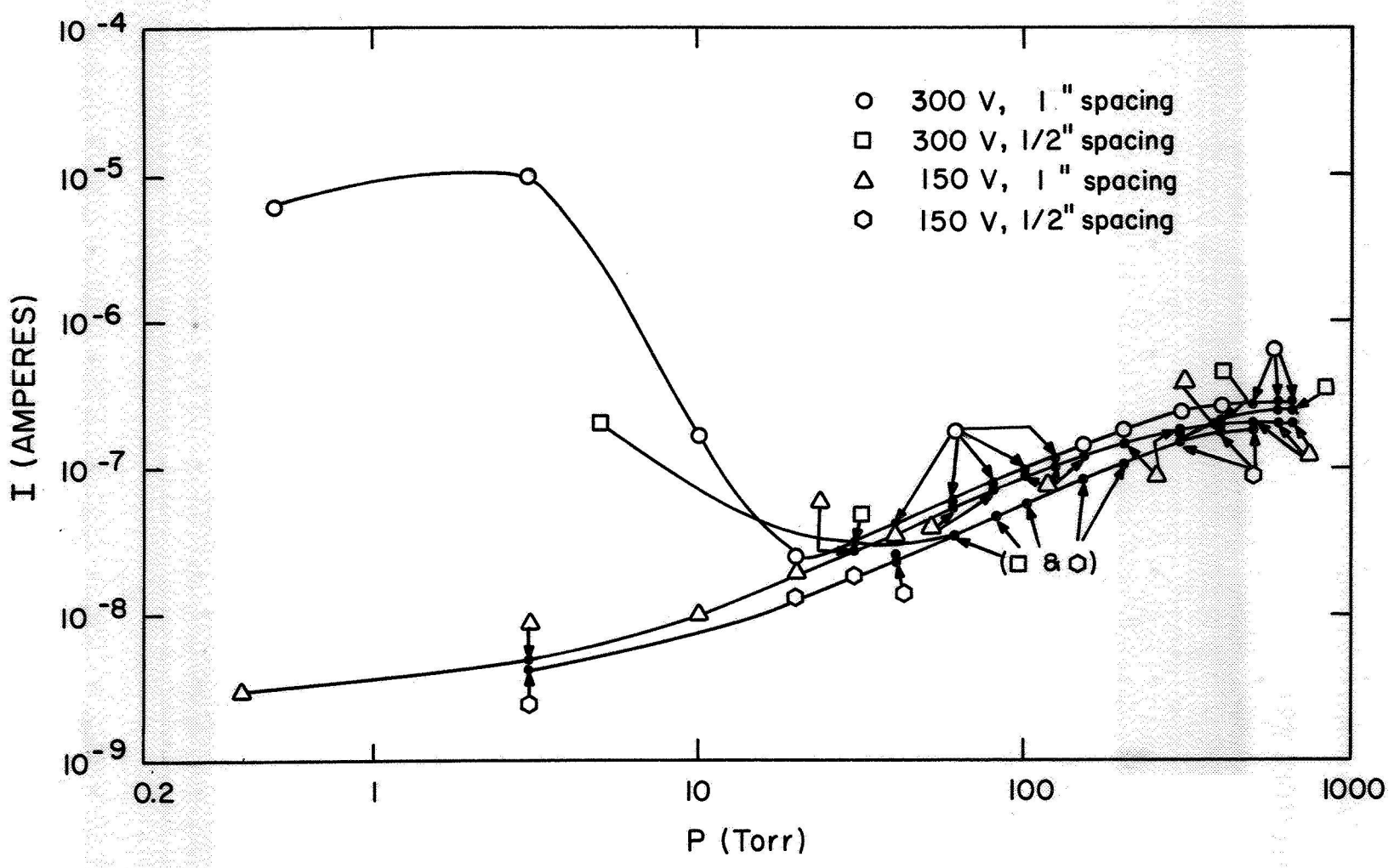

Figure 8. Ionization current I versus pressure P for pure argon at room temperature. Configuration was two circular parallel electrodes, one 2 7/8 in. in diameter and the other 3 3/8 in. in diameter. Two 1000 μCi sources were used, one mounted on each electrode.

strengths. The current maxima for low pressures at 300 V are caused by multiplication and will be discussed in the next section.

B. Proportional Counters

Measurements were made on a coaxial device having a copper wire central electrode (0.005 in. diameter) supported at both ends by glass-to-metal seals in a 7/16 in. i.d. brass tube of length 2 in. The 100 μCi Am-241 foil was curved and snug fit against the inside wall of the brass tube with a small wire spring clip. In an early experiment, the same current was measured both with and without guard rings under otherwise identical conditions, so we discontinued their use in later tests.

Data of current versus voltage for pure argon at four pressures are shown in Figure 9. At voltages below 100-200 V we see the now familiar ionization chamber behavior. Above 200 V multiplication sets in and the current rises sharply, attaining multiplications of over 10^4 at higher voltages. No attempt was made to determine the quantitative dependence of I on V and P. An important point is the cross-over of the four curves between 300 and 500 V. This indicates that above 500 V the current I increases as P decreases from 657 Torr to 20 Torr; at still lower pressures the current will decrease. Hence the variation of I with gas density at high voltages is not monotonic. Use of such a device as a gas density detector could lead to ambiguity unless the device were well calibrated.

Figure 10 and 11 show data on pure argon and on a 90% argon - 10% carbon dioxide mixture, at lower voltages. There is no apparent multiplication for P ~ 700 Torr at these voltages. We note the current maximum in pure argon near 4 Torr at 400 V, caused by multiplication at lower gas densities where

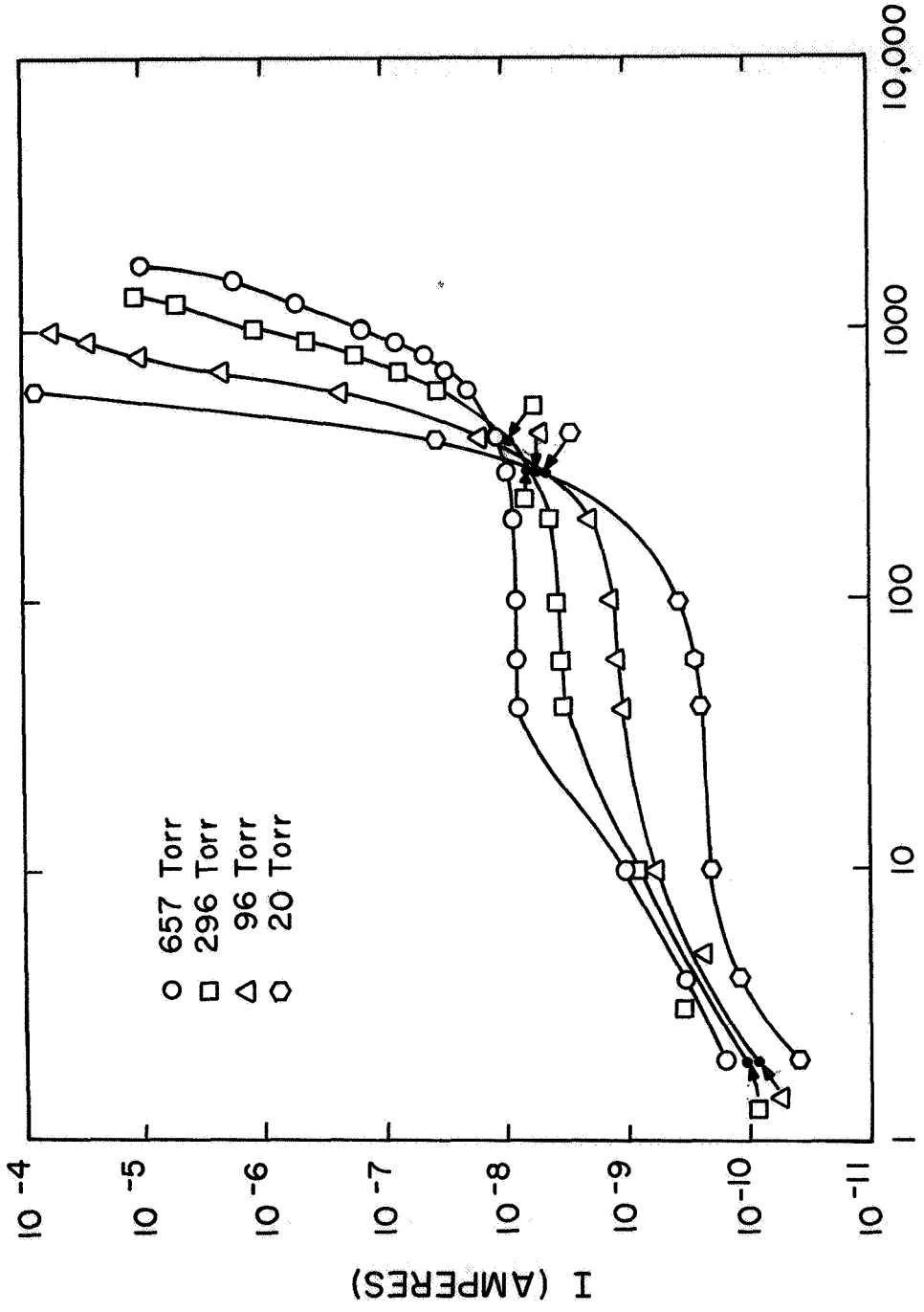

Figure 9. Current I versus voltage V for pure argon at room temperature. Configuration (see text) was coaxial with one 100 μCi Am-241 foil source.

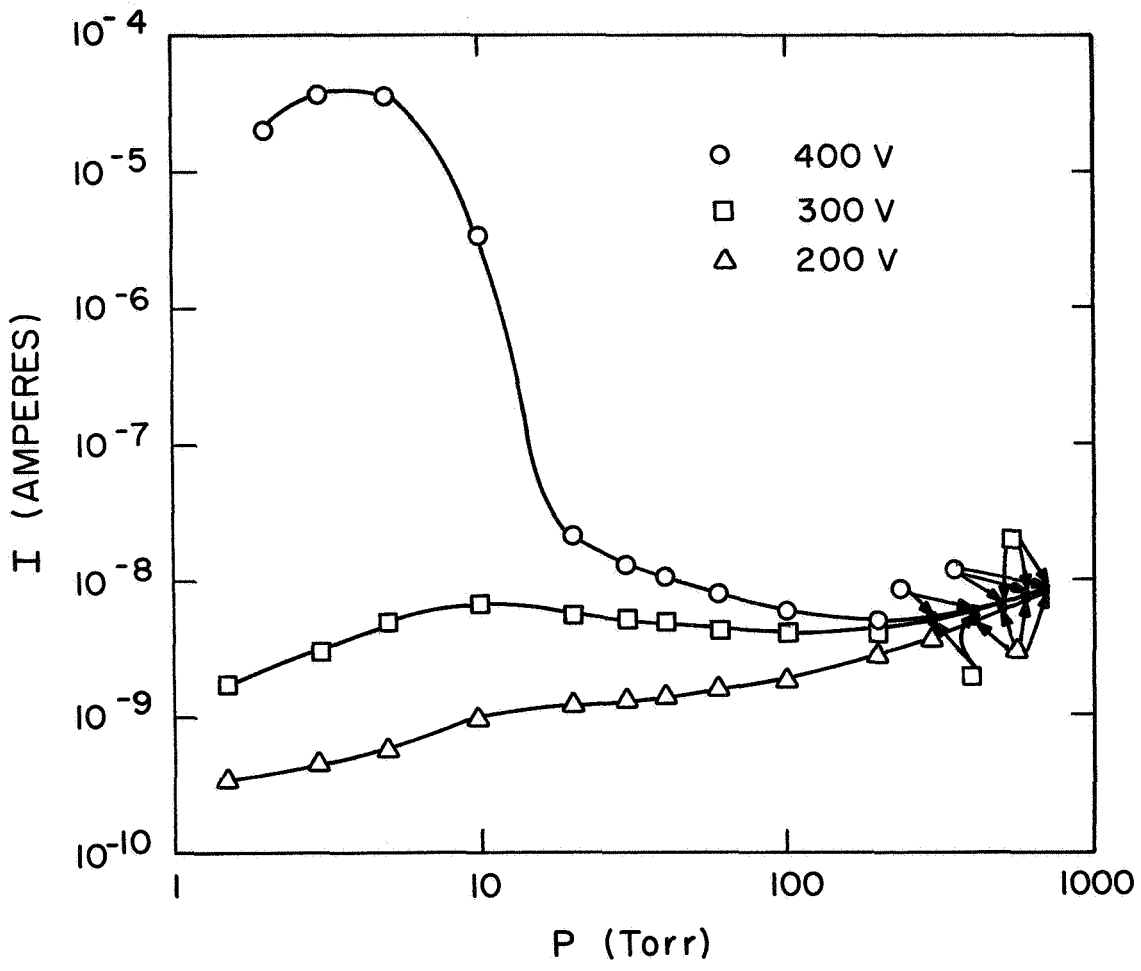

Figure 10. Current I versus pressure P for pure argon at room temperature. Same configuration as in Figure 9.

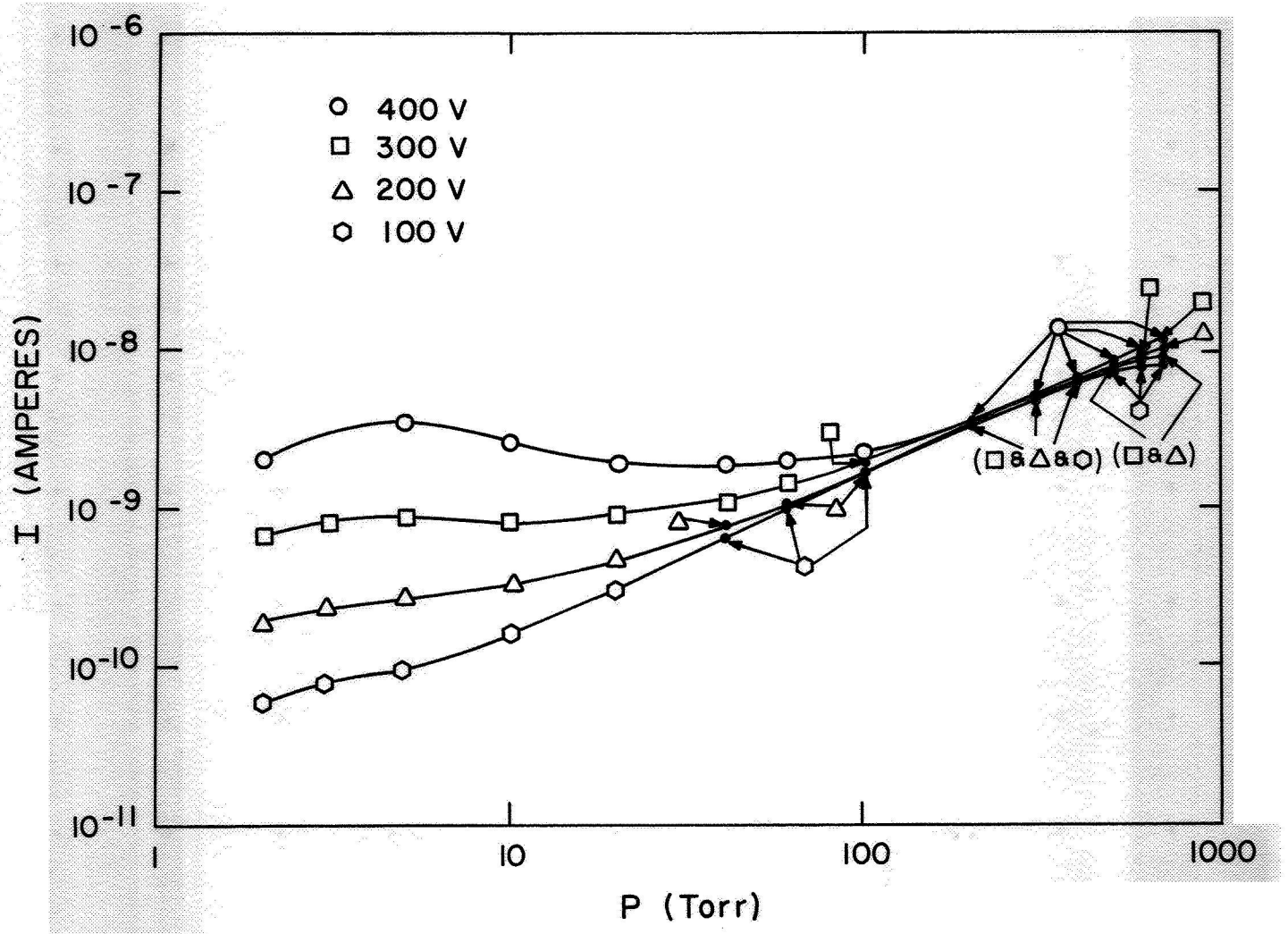

Figure 11. Current I versus pressure P for 90% argon - 10% CO_2 at room temperature. Same configuration as in Figure 9.

the electron mean free path becomes large. The addition of 10% CO_2 to argon lowers the electron agitation energy and decreases the multiplication, as we see in Figure 11. In both cases, however, there is some multiplication at lower pressures for voltages above 300 V, which is the same effect seen in Figure 8 for pure argon in the parallel plate geometry. We did not investigate the effect on I of variations in the tube geometry and the foil activity.

C. Glow Tubes

We have made extensive tests to determine the optimum design for a glow tube gas detector. Reported in this section are our preliminary tests and calibration data for our final design for a prototype gas detector. In principle, one should use careful cleaning and outgassing techniques, but time limitations forced us to compromise on some of these precautions. We found that molybdenum did not solder with tin, lead or silver solders using various acid fluxes. Therefore nickel wire has been used in all our designs (with one exception) since it is readily available and solders easily.

Preliminary data on some prototype detectors are shown in Figure 12 and Table VII. The vacuum chamber was flushed before each set of data was taken, but no heating or outgassing at high vacuum was attempted. Two parallel, cylindrical electrodes (each ~ 1/32 in. diam. and 5/16 in. in length, spaced ~ 1/16 in. apart) with a barium-strontium surface from a stripped-down commercial glow lamp were inserted in our vacuum chamber with 99% He - 1% A and tested for breakdown at various pressures. The results are shown in curve 1 in Figure 12, where one observes V_s^{min} to be 165 V at 20 Torr. A similar curve (not shown) for pure argon gas gave V_s^{min} as 160 V at 20 Torr. The other tests were performed with coaxial devices utilizing a brass tube

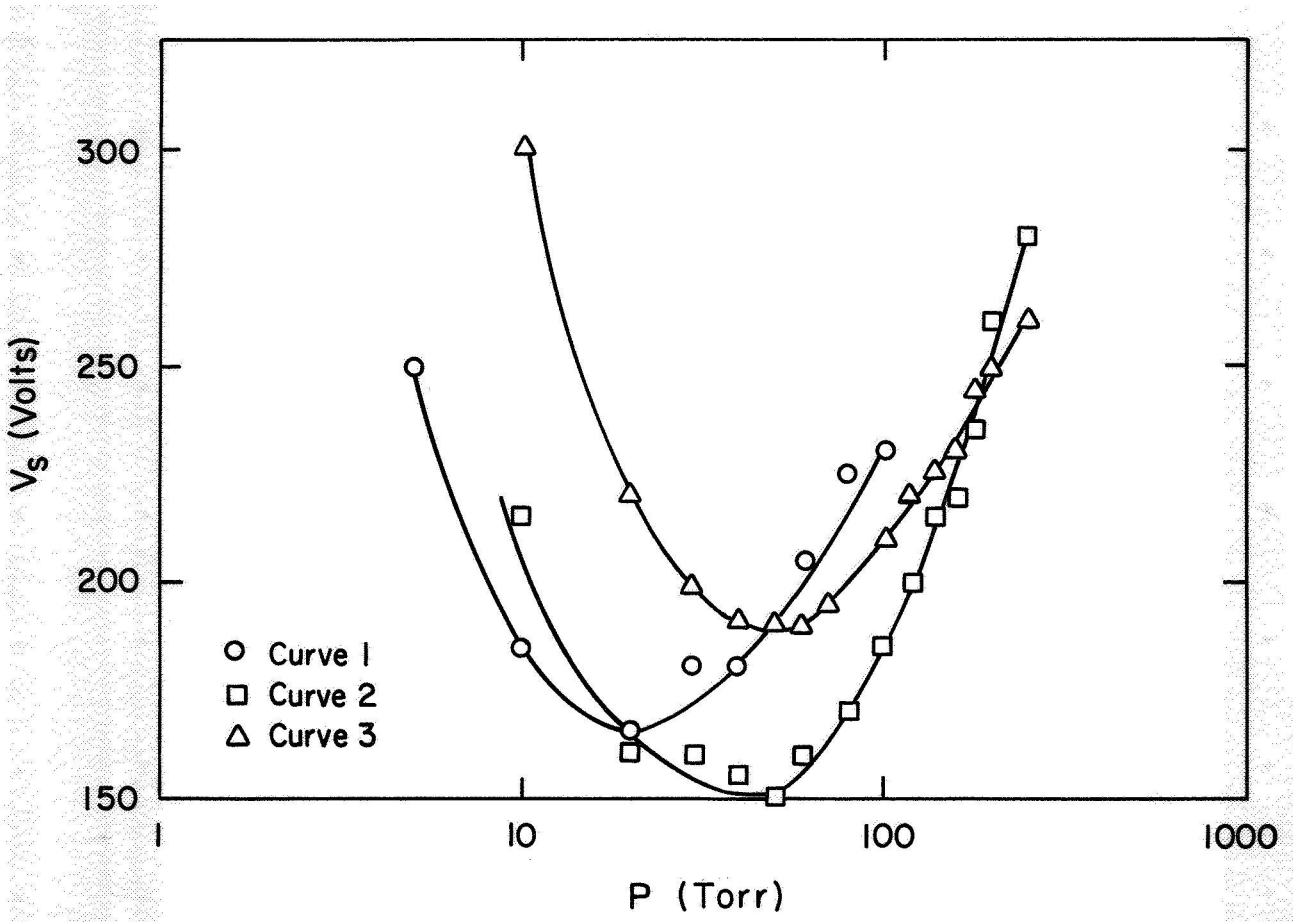

Figure 12. Striking voltage V_s versus pressure P at room temperature. Curve 1 is for two parallel, cylindrical electrodes from a commercial glow tube using 99% He - 1% A. Curve 2 is for a coaxial device described in the text with the central wire negative using pure helium gas. The data in curve 3 were taken for the same gas and configuration as curve 2 except that the central wire was positive.

(1/8 in. o.d. and 3/32 in. i.d.) and a nickel wire central electrode along the axis of the tube. The wire was led out of the brass tube either through a glass-to-metal seal (in the case of .020 in. nickel wire) or through a plastic insulator (in the case of .033 in. and .040 in. diam. nickel wires). The length of the brass tube and coaxial wire were the same. Curves 2 and 3 in Figure 12 show data for a device 1 in. in length with .020 in. diam. nickel wire in pure helium gas. The central wire electrode is negative in curve 2

Table VII. Minimum striking voltage V_s^{min} versus pressure P for several coaxial devices using pure helium gas. Configuration details are given in the text.

V_s^{min} (V)	P(Torr)	Length (in.)	Central Wire diam. (in.)	Central Wire Polarity
150	50	1	.020	-
190	40-60	1	.020	+
180	30-40	1/2	.020	-
190	50	1/2	.020	+
170	30-80	1/2	.033	-
180	50-80	1/2	.033	+
150	40-60	1/2	.040	-
190	50-120	1/2	.040	+

and positive in curve 3. An interesting point is that curve 3 crosses curve 2 at roughly 185 Torr. The lower V_s values for the positive central electrode at pressures above 185 Torr indicate the predominance of photoelectron production over electron production by positive ion bombardment of the cathode, and might be of use at high detector filling pressures. The minimum striking

voltage V_s^{min} for these two and several other similar coaxial configurations with pure helium gas are shown in Table VII. The data are roughly the same for different wire diameters, a result in agreement with theory.[10] V_s^{min} is lower when the central wire electrode is negative. We note that V_s^{min} is roughly the same (though higher than the values reported in the literature[10]) for the barium-strontium, commercial, cylindrical electrodes and for our coaxial nickel-brass devices, a fact probably explained by surface contamination of the electrodes. Other data showed little difference in V_s^{min} for a given coaxial device with 99% He - 1% A used instead of pure helium, probably due to gas contamination. By varying the external resistance in series with a glow tube, currents from 0.5 to 3.5 mA have been obtained, the tube voltage V_r remaining constant within 10%, as expected in the normal glow discharge region (E to F in Figure 2).

An alternative coaxial geometry similar to that shown in Figure 13 was designed. The central wire electrode is shorter than its coaxial brass tube, with a brass plug soldered into one end of the tube, while the wire comes out the other end through a glass-to-metal seal. The brass plug eliminates one glass-to-metal seal and provides a convenient place on which to solder a radioactive foil source. A gas feed tube on the side allows evacuation and filling. Data for several of these devices with a .025 in. diam. nickel wire in pure helium gas at 100 Torr pressure and room temperature are given in Table VIII. No cobalt-60 foils were used in these devices, and brass plugs were omitted on two of the detectors. The two main items of interest in this data are the lower values of V_s for the 3/32 in. i.d. brass tubes, and the higher values for the tubes with nickel wire central electrodes only 1/4 in. long. These data suggested our final design (see

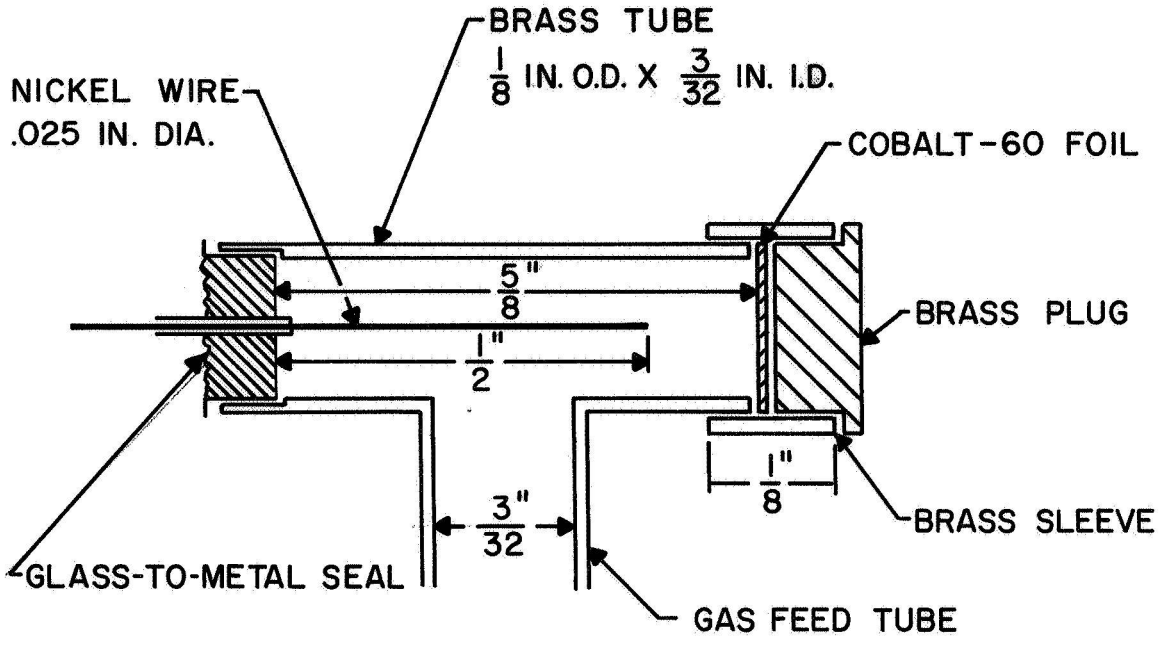

Figure 13. Final glow tube design.

Figure 13) of a 3/32 in. i.d. brass tube with a central electrode 1/2 in. in length.

Our final design for a prototype gas detector is shown in Figure 13. The Electrical Industries (691 Central Avenue, Murray Hill, New Jersey) Type 4AS-40T-SX, compression-type, glass-to-metal seal used there has a tubular central conductor through which the .025 in. diameter nickel wire passes and to which it is soldered. The cobalt foils were too large to fit in the 3/32 in. i.d. brass tube, so a 1/8 in. i.d. brass sleeve was used in combination with the brass plug to hold the foil in. The sleeve is only a characteristic of our prototype model and is not a necessary feature. All joints were soldered with pure tin solder. After construction each unit was cleaned off carefully and then washed (both inside and outside) successively with dilute nitric acid, distilled water and acetone.

Table VIII. Striking voltage V_s for several coaxial devices with pure helium at 100 Torr pressure and room temperature.

V_s (V)	Nickel Wire Length (in.)	Brass Tube Length (in.)	Brass Tube i.d. (in.)	Central Electrode Polarity	Brass Plug
240	1	1 1/8	1/8	-	Yes
240	1	1 1/8	1/8	+	Yes
232	1/2	5/8	1/8	-	Yes
257	1/2	5/8	1/8	+	Yes
310	1/4	5/16	1/8	-	Yes
277	1/4	5/16	1/8	+	Yes
220	1/2	3/4	3/32	-	No
210	1/2	3/4	3/32	+	No

Ten cobalt-59 foils, each ≈ 1/8 in. square by .005 in. thick and weighing 6 mg, were irradiated with thermal neutrons in the VPI reactor in order to activate cobalt-60. The foils had measured activities between 0.32 and 0.37 μCi after irradiation. Cobalt-60 has a half-life $T_{1/2}$ of 5.3 years, emitting a beta particle (314 keV maximum kinetic energy) and two gamma rays (1.173 MeV and 1.332 MeV). After a foil was installed in a detector as in Figure 13, the measured radiation outside the detector was 3 to 4 millirem/hr (a typical luminiscent wrist watch gives out 1 to 2 millirem/hr). Cobalt-60 unsealed foils of this low activity (< 1 μCi) do not require an AEC license and up to ten of them can be sent through the mail to an unlicensed party. However, in the interests of safety, reasonable precautions should be used in handling these detectors.

Calibration data for units constructed in our final design (Figure 13) are given in Tables IX and X and in Figure 14. The units are designated #1, #2 and #3. The data were taken with the devices either inside a bell jar vacuum system or, when using a temperature bath, soldered onto a tube connected to the vacuum system. These units were not heated or outgassed at high vacuum prior to testing. The measurements of V_s and I for unit #2 show (Table X) that there was no great variation between 0^o and 100^o C. However, the striking voltage V_s did rise by 50 to 100 V at liquid air temperatures (-195^o C) compared to room temperature. Comparison of the data at room temperature for the three units gives an idea of the variation in characteristics from unit to unit. The voltage-current characteristic in Figure 14 is unlike previous measurements in that it is not flat and the voltage variations exceed 10%. We have no explanation for these results. If the applied voltage was kept constant and the helium gas pressure was slowly lowered (at fixed temperature), the current remained constant within

Table IX. Striking voltage V_s, current I and pressure P for units #1 and #3 with pure helium at room temperature. Polarity is that of the central wire electrode. A 46 kilohm resistor was in series with the tube.

P(Torr)	Unit #1 (+ Polarity) V_s(V)	I(mA)	Unit #1 (- Polarity) V_s(V)	I(mA)	Unit #3 (- Polarity) V_s(V)	I(mA)
200	300	2.4	270	2.1	250	1.8
175	280	2.0	260	1.7	230	1.4
150	270	1.6	250	1.6	210	1.1
125	230	1.0	210	1.0	-	-
100	200	0.52	200	0.80	200	1.0
75	210	0.60	190	0.40	170	0.60
50	180	0.28	180	0.54	180	0.80
25	230	0.60	180	0.24	-	-

Table X. Striking voltage V_s, current I and pressure P for unit #2 with pure helium at four temperatures. The central wire electrode had negative polarity. A 46 kilohm resistor was in series with the tube.

P(Torr)	100° C V_s(V)	I(mA)	22° C V_s(V)	I(mA)	0° C V_s(V)	I(mA)	-195° C V_s(V)	I(mA)
200	270	1.2	270	2.0	260	1.6	340	1.8
175	240	1.0	260	1.8	230	1.1	300	0.90
150	235	0.90	250	1.5	210	0.80	310	1.2
100	210	0.50	220	0.80	190	0.45	300	0.90
50	250	0.60	210	0.60	210	0.50	280	0.70

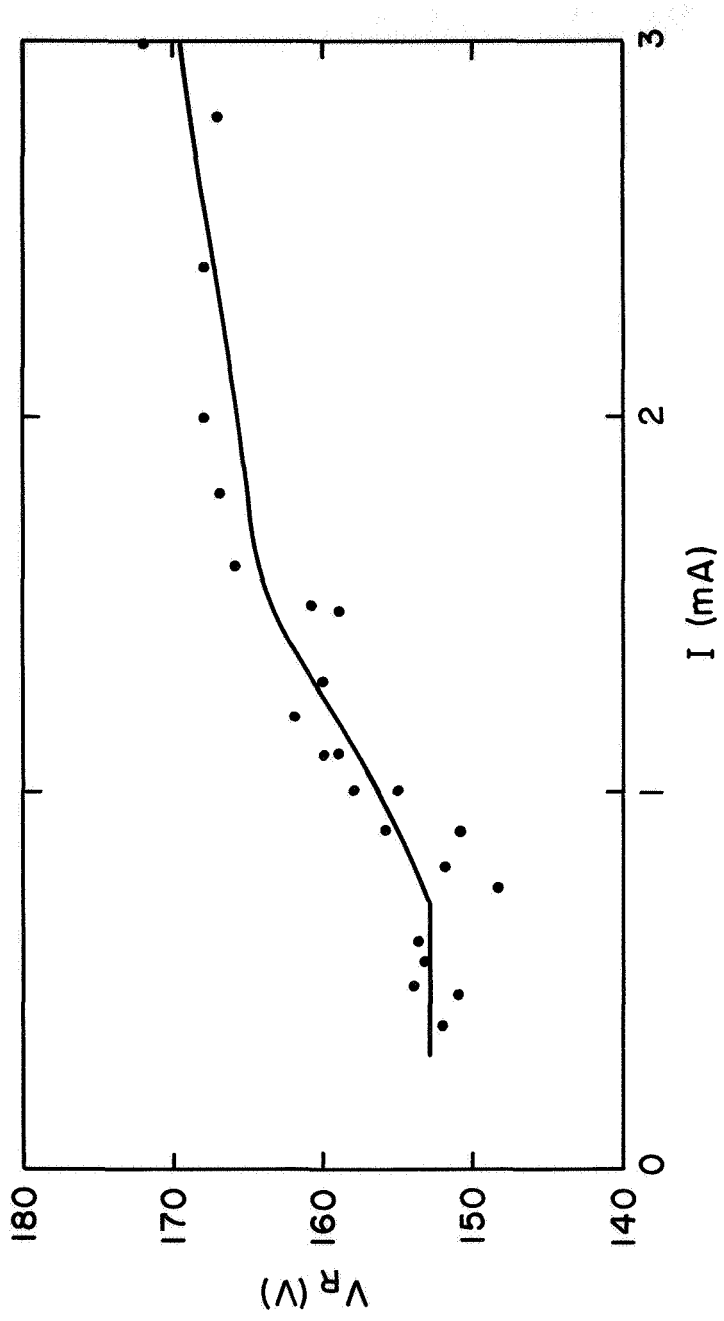

Figure 14. Running voltage V_R versus current I for unit #2 with pure helium at 100 Torr and room temperature.

a factor of 2 or 3 from 200 Torr to 20 Torr, and then dropped fairly rapidly to an extremely low value at about 15 Torr.

Unit #1 was installed in a calibrated vibrator in the VPI Engineering Mechanics Department, and subjected to oscillatory vibrations with the following maximum accelerations: 3g(18 Hz), 34g(500 Hz), 14g(1000 Hz), 1g(10,000 Hz) and 1g(20,000 Hz), where g is the acceleration due to gravity. Vibration at each frequency lasted five minutes. Values of V_s and I measured after the vibration treatment were essentially the same as those before, thereby showing that the unit can withstand these vibrations.

Our data on the effect of the cobalt-60 foil source show some inconsistencies, but the trend is clear. One device was constructed exactly like unit #1 except without the Co-60 foil in it. With the central electrode negative, V_s was 50 to 100 V higher than in unit #1 at helium pressures between 25 and 100 Torr at room temperature, but was the same at 150 Torr. Another effect we have observed is that the striking voltage rose if the unit was left in the bell jar at a given gas pressure. The rise was ~ 40 V in 4 hours and ~ 100 V in 10 hours for one unit without a Co-60 foil. Another identical unit with a Co-60 foil in it showed a rise of only 40 V in 10 hours.

Unit #3 was tested with our limited supply of pure neon gas, and gave similar characteristics to the helium; V_s was 190-200 V for neon pressures between 25 and 100 Torr at room temperature. Hence our devices have roughly the same characteristics for pure helium, pure neon, and for 99% He - 1% A, in disagreement with theory. This may have been caused by outgassing from the walls of our vacuum system.

Attempts were made to construct a sealed detector, i.e., to seal off

the gas feed tube with, say, helium gas at 100 Torr in the detector. Due to time limitations we were not able to perfect our technique for sealing off the feed tube. A series of five sealed detectors were constructed, but none worked. Prior to filling and sealing, we baked the devices at 175^{o} F for two hours in the middle of a fifteen hour stretch during which they were outgassed in a high vacuum system.

V. CONCLUSIONS AND RECOMMENDATIONS

Our theoretical arguments and experimental results for ionization chambers are in agreement in giving maximum saturation currents ~ 10^{-7} – 10^{-6} A for reasonable radioactive source activities (~ 1 mCi alpha source) at several hundred volts. Since such low currents are difficult to detect under flight conditions in space, we cannot recommend ionization chambers for gas density detection. However, we draw attention to the approximate linear dependence of the current on gas density at intermediate densities, a fact which could be of use in a hole size detector if small currents were easily measurable in space.

Proportional counters provide currents up to 10^{-5} – 10^{-4} A at voltages ~ 1000 V, both of which compare unfavorably with typical glow tube characteristics. In addition, the proportional counter current is a non-monotonic function of the gas density at the high voltages required for significant multiplication, so that analysis of the counter output becomes difficult. The proportional counter is the least attractive candidate for gas density detection in space.

The most promising detector is one based on the glow tube. Currents ~ 1 mA at voltages ~ 200 V are attainable using helium or neon with filling pressures of 50 to 100 Torr at room temperature. These devices work in the temperature range -195° C to 100° C, but their striking voltage is 50% larger at -195° C than at room temperature. They can withstand strains from vibrations. This device appears to be most useful as an "on-off" type gauge, but may be difficult to use for hole size detection.[26] Calibration of a device used for the latter application would be complicated unless one could eliminate the change of the glow tube characteristics in time which we observed.

Our striking voltages increased 20% to 50% if the device sat in a bell jar chamber for 10 hours. This may have been due to outgassing from the vacuum system walls. Careful cleaning and outgassing of these devices should help this problem. The cobalt-60 foil sources (0.34 μCi activity) reduced the effect in our work.

Finally, we indicate some modifications that might be worth studying in further work. Ceramic seals have better vibration and temperature characteristics than glass-to-metal seals and may be better for use in space. If a suitable means of welding or soldering molybdenum can be found, this may be a superior central electrode material. A .006 or .008 in. thick nickel or molybdenum tube would probably be better for the outer electrode than the thicker brass tube used in our prototype glow tube device.

REFERENCES

1. W. A. Cosby and R. G. Lyle, The Meteoroid Environment and its Effect on Materials and Equipment, NASA SP-78 (U. S. Government Printing Office, Washington, D. C., 1965).

2. H. W. Fulbright, "Ionization Chambers in Nuclear Physics", in Handbuch der Physik (Springer Verlag, Berlin, 1958), vol. 45, pp. 1-51.

3. B. Rossi and H. Staub, Ionization Chambers and Counters (McGraw-Hill, New York, 1949).

4. H. Staub, "Detection Methods", in E. Segre, editor, Experimental Nuclear Physics (John Wiley & Sons, New York, 1953), vol. 1, pp. 1-165.

5. W. Franzen and L. W. Cochran, "Pulse Ionization Chambers and Proportional Counters", in A. H. Snell, editor, Nuclear Instruments and Their Uses (John Wiley & Sons, New York, 1962), vol. 1, pp. 3-81.

6. M. A. El-Moslimany, Theoretical and Experimental Investigation of Radioactive Ionization Gauges, Scientific Report No. HS-1, University of Michigan Research Institute, Ann Arbor, 1960 (unpublished).

7. E. Segre, Nuclei and Particles (W. A. Benjamin, New York, 1965).

8. S. C. Curran, "The Proportional Counter as Detector and Spectrometer", in Handbuch der Physik (Springer Verlag, Berlin, 1958), vol. 45, pp. 174-221.

9. S. A. Korff, "Geiger Counters", in Handbuch der Physik (Springer Verlag, Berlin, 1958), vol. 45, pp. 52-85.

10. J. R. Acton and J. D. Swift, Cold Cathode Discharge Tubes (Academic Press, New York, 1963).

11. F. Llewellyn-Jones, Ionization and Breakdown in Gases (John Wiley and Sons, New York, 1957).

12. S. Flugge, editor, Gas Discharges II, Handbuch der Physik (Springer Verlag, Berlin, 1956), vol. 22.

13. J. Millman, Vacuum Tube and Semiconductor Electronics (McGraw-Hill, New York, 1958), Chap. 12 and 13.

14. Glow Lamp Manual, Second Edition (General Electric Company, Nela Park, East Cleveland, Ohio, 1966).

15. H. A. Bethe and J. Ashkin, "Passage of Radiations through Matter", in E. Segre, editor, Experimental Nuclear Physics (John Wiley and Sons, New York, 1953), vol. 1, pp. 166-357.

16. E. A. Uehling, "Penetration of Heavy Charged Particles in Matter", in Annual Reviews of Nuclear Science, vol. 4, pp. 315-350 (1954).

17. E. A. Uehling, editor, Penetration of Charged Particles in Matter (National Academy of Sciences-National Research Council Publication 752, Washington, D. C., 1960, unpublished).

18. Studies in Penetration of Charged Particles in Matter (National Academy of Sciences - National Research Council Publication 1133, Washington, D. C., 1964, unpublished).

19. J. E. Turner, in reference 18, pp. 99-101.

20. W. P. Trower, UCRL-11647 (Rev.), University of California, Berkeley, 1966 (unpublished).

21. W. P. Trower, UCRL-2426 (Rev.), vol. II, and UCRL-2426, vol. IV, University of California, Berkeley, 1966 (unpublished).

22. See, for example, J. L. Sommerville, editor, The Isotope Index (Scientific Equipment Company, P. O. Box 19086, Indianapolis, Indiana, 1967).

23. F. L. Torney, Jr., "Investigation of a Replacement Source for the Alphatron Measuring System", Final Report for NASA Contract NAS1-2691-3, 1964, (unpublished).

24. C. Kittel, Introduction to Solid State Physics, Third Edition (John Wiley & Sons, New York, 1966), pp. 215-218.

25. L. I. Schiff, Quantum Mechanics, Third Edition (McGraw-Hill, New York, 1968), pp. 123-124.

26. L. McMaster of NASA-Langley Research Center (Hampton, Va.) has informed us that a hole size detector based on the variation of V_s with gas density is feasible, and that laboratory prototypes are operational.